

Haldane-gap chains in a magnetic field

Fabian H.L. Essler^(a) and Ian Affleck^(b)

^(a) *The Rudolf Peierls Centre for Theoretical Physics, Oxford University, Oxford OX1 3NP, UK*

^(b) *Department of Physics and Astronomy, University of British Columbia, Vancouver, B.C., Canada V6T 1Z1*

We consider quasi one dimensional spin-1 Heisenberg chains with crystal field anisotropy in a uniform magnetic field. We determine the dynamical structure factor in various limits and obtain a fairly complete qualitative picture of how it changes with the applied field. In particular, we discuss how the width of the higher energy single magnon modes depends on the field. We consider the effects of a weak interchain coupling. We discuss the relevance of our results for recent neutron scattering experiments on the quasi-1D Haldane-gap compound NDMAP.

I. INTRODUCTION

Recent years have seen a resurgence of interest in field-induced “magnon condensation” in gapped quasi one-dimensional quantum antiferromagnets. In particular a series of ESR and neutron scattering experiments have been carried out on the Haldane-gap¹ chain compounds NDMAP²⁻⁷ and NDMAZ⁸. The main motivation for these experimental studies is the observation that a spin-1 Heisenberg chain undergoes a quantum phase transition between a gapped spin-liquid phase and a gapless Luttinger liquid phase at some critical value H_c of the applied magnetic field H ^{9,10}. The ground state of the spin-1 Heisenberg chain is a spin singlet and excitations are described in terms of a gapped $S = 1$ triplet of magnons. When a magnetic field is applied, the triplet splits due to the Zeeman effect and one of the magnon gaps is driven to zero at H_c . For $H > H_c$ the ground state is magnetized and excitations are gapless. If interactions between the magnons were absent, the transition at H_c could be understood as a Bose-Einstein condensation of magnons. In the spin-1 Heisenberg chain there is an interaction between magnons, which fundamentally changes the ground state for $H > H_c$ from a condensate of bosonic magnons to a Luttinger liquid, which can be regarded as a one dimensional version of an interacting Bose condensate. The transition at $H = H_c$ is in the universality class of the commensurate-incommensurate (C-IC) phase transition¹¹. The magnetic response of the isotropic spin-1 chain in strong fields $H > H_c$ has been analyzed in some detail in Refs [12–14]. In Appendix A we use the nonlinear sigma model description of the isotropic spin-1 chain to derive explicit expressions for the dynamical response functions in the low-field phase $H < H_c$. In many $S = 1$ compounds such as NENP, NDMAP and NDMAZ strong crystal field anisotropies are present, which lead to a zero-field splitting of the magnon triplet comparable in magnitude to the Haldane gap itself. These anisotropy effects lead to more complex behavior and a richer phase diagram. The purpose of this work is to determine the dynamical response of Haldane-gap compounds in the presence of such crystal field anisotropies. The relevant lattice Hamiltonian is of the form

$$\begin{aligned} \mathcal{H} = & J \sum_j \mathbf{S}_j \cdot \mathbf{S}_{j+1} - \mathbf{H} \cdot \mathbf{S}_j \\ & + \sum_j D(S_j^z)^2 + E[(S_j^x)^2 - (S_j^y)^2], \end{aligned} \quad (1.1)$$

where $0 < -E < D$. In zero field there are three magnon modes in the vicinity of the antiferromagnetic wave number $q = \frac{\pi}{a_0}$ with gaps $\Delta_1 < \Delta_2 < \Delta_3$. For simplicity we will mainly concentrate on the case where the magnetic field is applied along the z-axis, i.e.

$$\mathbf{H} = H\vec{e}_z. \quad (1.2)$$

The lattice Hamiltonian (1.1) (with field applied along the z-direction) exhibits two discrete symmetries which play an important role in the following:

1. Rotation by π around the z-axis (\mathbf{R}_π^z):

$$S_j^x \rightarrow -S_j^x, \quad S_j^y \rightarrow -S_j^y, \quad S_j^z \rightarrow S_j^z. \quad (1.3)$$

2. Translation by one site (\mathbf{T}_R):

$$S_j^\alpha \rightarrow S_{j+1}^\alpha, \quad \alpha = x, y, z. \quad (1.4)$$

The model (1.1) is difficult to analyze directly by analytical methods. However, progress can be made by concentrating on the low-energy regime, which can be studied by means of semi-phenomenological descriptions in terms of continuum models. Two such models have been used in particular, namely (i) a bosonic Landau-Ginzburg model^{10,14} and (ii) a theory of three coupled Majorana fermions¹⁵. In the present work we go beyond the original works^{10,14,15} by (1) discussing the decay of high energy magnon modes, (2) applying methods of integrable quantum field theory to the discussion of structure functions and (3) taking into account the effects of inter-chain interactions.

The outline of this paper is as follows. We start by reviewing known results on the spectrum of the Majorana fermion model in section II B. We then investigate the role played by interactions in sections II C and II D and in particular show that interactions generate a finite lifetime for one of the magnon modes. In section III we derive analogous results in the framework of the Landau-Ginzburg theory. We then turn to a more detailed analysis of the magnetic response functions in the low-energy regime in the vicinity of the quantum critical point at H_c in section IV. Section V gives a detailed account of the low-energy regime in the high-field phase for small crystal-field anisotropy. The effects of interchain coupling are investigated in section VI and a summary and discussion of our various results is given in section VII. A variety of technical details are presented in Appendices A-E.

II. MAJORANA FERMION MODEL

In Ref.[15] A.M. Tselik proposed a description of the spin-1 Heisenberg chain in terms of a field theory of three right and left moving Majorana (real) fermions $R_a = R_a^\dagger$, $L_a = L_a^\dagger$, $a = 1, 2, 3$. The Hamiltonian is given by

$$\begin{aligned} \mathcal{H} = & \frac{i}{2} \sum_{a=1}^3 v [L_a \partial_x L_a - R_a \partial_x R_a] - \Delta_a [R_a L_a - L_a R_a] \\ & + \frac{i}{2} \sum_{a,b,c} \varepsilon^{abc} H_a (L_b L_c + R_b R_c) + \mathcal{H}' , \end{aligned} \quad (2.1)$$

where \mathcal{H}' describes anisotropic current-current interactions

$$\mathcal{H}' = \sum_a g_a J^a J^a . \quad (2.2)$$

Here the currents are bilinears in the Majorana fermions

$$J^a(x) = -\frac{i}{2} \varepsilon^{abc} [L_b L_c + R_b R_c] . \quad (2.3)$$

We will take the magnetic field along the 3-axis and concentrate on the case

$$\Delta_1 < \Delta_2 < \Delta_3 . \quad (2.4)$$

The generalization of our results to other situations is straightforward. The smooth and staggered components of the spin operators are defined by the decomposition

$$S_j^\alpha \longrightarrow J^\alpha(x) + (-1)^j n^\alpha(x) , \quad (2.5)$$

where $x = ja_0$. The smooth components are equal to the currents, where $a = 1, 2, 3$ correspond to $\alpha = x, y, z$. The staggered components are expressed in terms of Ising order and disorder operators

$$\begin{aligned} n^x(x) & \propto \sigma^1(x) \mu^2(x) \mu^3(x) , \\ n^y(x) & \propto \mu^1(x) \sigma^2(x) \mu^3(x) , \\ n^z(x) & \propto \mu^1(x) \mu^2(x) \sigma^3(x) . \end{aligned} \quad (2.6)$$

We note that the signs of the mass terms in (2.1) are such that in zero field

$$\langle \sigma^a(x) \rangle = 0 , \quad \langle \mu^a(x) \rangle \neq 0 . \quad (2.7)$$

A. Symmetries

The Hamiltonian (2.1) inherits the discrete symmetries \mathbf{T}_R and \mathbf{R}_π^z from the lattice model. The latter is realized as

$$\begin{aligned} \mathbf{R}_\pi^z : \quad R_a &\longrightarrow -R_a, \quad L_a \longrightarrow -L_a, \\ \sigma^a &\longrightarrow -\sigma^a, \quad \mu^a \longrightarrow \mu^a, \quad a = 1, 2. \end{aligned} \quad (2.8)$$

The translation symmetry by one site turns into a discrete Z_2 symmetry in the continuum limit

$$J^a(x) \longrightarrow J^a(x), \quad n^a(x) \longrightarrow -n^a(x), \quad (2.9)$$

and may be realized as

$$\begin{aligned} R_a &\longrightarrow -R_a, \quad L_a \longrightarrow -L_a, \\ \sigma^a &\longrightarrow -\sigma^a, \quad \mu^a \longrightarrow \mu^a, \quad a = 1, 2, 3. \end{aligned} \quad (2.10)$$

It is convenient to combine this symmetry with \mathbf{R}_π^z into the following Z_2 symmetry

$$\begin{aligned} \mathbf{T}_R \mathbf{R}_\pi^z : \quad R_3 &\longrightarrow -R_3, \quad L_3 \longrightarrow -L_3, \\ \sigma^3 &\longrightarrow -\sigma^3, \quad \mu^3 \longrightarrow \mu^3. \end{aligned} \quad (2.11)$$

The full symmetry of the Majorana model (2.1) is thus $Z_2 \otimes Z_2$.

B. Spectrum in the absence of interactions

In the absence of interactions, i.e. $g_a = 0$ in (2.2) the Hamiltonian can be diagonalized by means of a Bogoliubov transformation¹⁵. In the following we review some relevant formulas. As the magnetic field is along the 3-direction only the first and second Majoranas couple to the magnetic field. The third Majorana gives rise to a fermionic single-particle mode with dispersion

$$\omega_3(k) = \sqrt{\Delta_3^2 + v^2 k^2}. \quad (2.12)$$

The first and second Majoranas are conveniently combined into a complex fermion Ψ

$$\begin{aligned} R_1 &= \frac{\Psi_R + \Psi_R^\dagger}{\sqrt{2}}, \quad R_2 = \frac{\Psi_R - \Psi_R^\dagger}{i\sqrt{2}}, \\ L_1 &= \frac{\Psi_L + \Psi_L^\dagger}{\sqrt{2}}, \quad L_2 = \frac{\Psi_L - \Psi_L^\dagger}{i\sqrt{2}}. \end{aligned} \quad (2.13)$$

The Hamiltonian density describing the first and second Majoranas takes the form

$$\begin{aligned} \mathcal{H}_{12} &= -iv \left[\Psi_R^\dagger \partial_x \Psi_R - \Psi_L^\dagger \partial_x \Psi_L \right] \\ &\quad + \frac{H}{2} \left[[\Psi_R^\dagger, \Psi_R] + [\Psi_L^\dagger, \Psi_L] \right] \\ &\quad - im \left[\Psi_R^\dagger \Psi_L - h.c. \right] + i\Delta \left[\Psi_R^\dagger \Psi_L^\dagger - h.c. \right], \end{aligned} \quad (2.14)$$

where

$$\Delta = \frac{\Delta_2 - \Delta_1}{2}, \quad m = \frac{\Delta_2 + \Delta_1}{2}. \quad (2.15)$$

Introducing a mode expansion

$$\begin{aligned} \Psi_R(x) &= \int_0^\infty \frac{dk}{2\pi} \left[e^{ikx} \alpha(k) + e^{-ikx} \beta^\dagger(k) \right], \\ \Psi_L(x) &= \int_{-\infty}^0 \frac{dk}{2\pi} \left[e^{ikx} \alpha(k) + e^{-ikx} \beta^\dagger(k) \right], \end{aligned} \quad (2.16)$$

we may express the Hamiltonian density (2.14) as

$$H_{12} = \int_0^\infty \frac{dk}{2\pi} \sum_{a,b=1}^4 \gamma_a^\dagger(k) M_{ab} \gamma_b(k), \quad (2.17)$$

where

$$\gamma_a(k) = (\alpha(k), \alpha^\dagger(-k), \beta(k), \beta^\dagger(-k))_a, \\ M = \begin{bmatrix} vk + H & i\Delta & 0 & -im \\ -i\Delta & -vk - H & im & 0 \\ 0 & -im & vk - H & i\Delta \\ im & 0 & -i\Delta & -vk + H \end{bmatrix}. \quad (2.18)$$

Now we perform a Bogoliubov transformation with a unitary matrix $U(k)$

$$\begin{pmatrix} c_+(k) \\ c_+^\dagger(-k) \\ c_-(k) \\ c_-^\dagger(-k) \end{pmatrix} = U(k) \begin{pmatrix} \alpha(k) \\ \alpha^\dagger(-k) \\ \beta(k) \\ \beta^\dagger(-k) \end{pmatrix}, \quad (2.19)$$

to bring H_{12} to a diagonal (normal ordered) form

$$H_{12} = \int_{-\infty}^\infty \frac{dk}{2\pi} \sum_{a=\pm} \omega_a(k) c_a^\dagger(k) c_a(k), \\ \omega_\pm(k) = \left[m^2 + \Delta^2 + H^2 + v^2 k^2 \pm 2\sqrt{m^2 \Delta^2 + H^2(m^2 + v^2 k^2)} \right]^{\frac{1}{2}}. \quad (2.20)$$

The gap $\omega_+(0)$ increases monotonically with H , whereas $\omega_-(0)$ decreases and vanishes at a critical field

$$H_c = \sqrt{\Delta_1 \Delta_2} = \sqrt{m^2 - \Delta^2}. \quad (2.21)$$

The corresponding critical point is in the Ising universality class. For fields $H < H_{c2}$

$$H_{c2} = m \left[\frac{1}{2} + \sqrt{\frac{1}{4} + \frac{\Delta^2}{m^2}} \right]^{\frac{1}{2}} \quad (2.22)$$

the minimum of the dispersion $\omega_-(k)$ occurs at $k = 0$. In the vicinity of H_c and at small momenta the dispersion is approximated as

$$\omega_-^2(k) \approx \frac{H_c^2}{m^2} (H - H_c)^2 + v^2 \left[\frac{\Delta^2}{m^2} + \frac{H_c(1 + \frac{\Delta^2}{m^2})}{m^2} (H_c - H) \right] k^2. \quad (2.23)$$

Hence the gap vanishes linearly with $H - H_c$ in agreement with Ising critical behaviour

$$\omega_-(0) \simeq (H - H_c) \sqrt{1 - \frac{\Delta^2}{m^2}}. \quad (2.24)$$

In order to see the Ising criticality described by (2.23) the magnetic field must be sufficiently close to H_c

$$H - H_c < \frac{\Delta^2}{H_c(1 + \frac{\Delta^2}{m^2})}. \quad (2.25)$$

As expected this scale is set by the anisotropy Δ . For $H > H_{c2}$ there are two degenerate minima of $\omega_-(k)$ at some incommensurate wave numbers $\pm k_F$ with

$$\begin{aligned} vk_F &= \left[H^2 - m^2 - \frac{m^2 \Delta^2}{H^2} \right]^{\frac{1}{2}}, \\ \omega_-(k_F) &= \Delta \sqrt{1 - \frac{m^2}{H^2}}. \end{aligned} \quad (2.26)$$

For $k \approx \pm k_F$ we have

$$\omega_-^2(k) \approx \Delta^2 \left[1 - \frac{m^2}{H^2} \right] + \left[\frac{v^2 k_F}{H} \right]^2 (|k| - k_F)^2. \quad (2.27)$$

As was recently pointed out by Wang²⁶, these results for the dispersions suggest that a cross-over between Ising and C-IC critical behaviour occurs as a function of H . For H very close to H_c we encounter Ising critical behaviour, which crosses over to C-IC behaviour for $H > H_{c2}$.

C. Interactions: self-consistent mean-field treatment

So far we have neglected the four-fermion interactions (2.2) altogether. As a first step of taking interactions into account we may treat them in a self-consistent mean-field approximation (SCMF). The following expectation values are compatible with the discrete Z_2 symmetries

$$\begin{aligned} \langle L_a R_a \rangle &\neq 0, \quad \langle L_1 L_2 \rangle \neq 0, \quad \langle R_1 R_2 \rangle \neq 0, \\ \langle R_1 L_2 \rangle &\neq 0, \quad \langle R_2 L_1 \rangle \neq 0. \end{aligned} \quad (2.28)$$

Decoupling the four fermion terms leads to a renormalization of the mass parameters

$$\begin{aligned} \Delta_1 &\longrightarrow \tilde{\Delta}_1 = \Delta_1 - 2ig_2 \langle L_3 R_3 \rangle - 2ig_3 \langle L_2 R_2 \rangle, \\ \Delta_2 &\longrightarrow \tilde{\Delta}_2 = \Delta_2 - 2ig_1 \langle L_3 R_3 \rangle - 2ig_3 \langle L_1 R_1 \rangle, \\ \Delta_3 &\longrightarrow \tilde{\Delta}_3 = \Delta_3 - 2ig_3 \langle L_2 R_2 \rangle - 2ig_2 \langle L_1 R_1 \rangle. \end{aligned} \quad (2.29)$$

The magnetic field terms are changed to

$$H_L L_1 L_2 + H_R R_1 R_2, \quad (2.30)$$

where $H_L = H + 2ig_3 \langle R_1 R_2 \rangle$. and $H_R = H + 2ig_3 \langle L_1 L_2 \rangle$. Finally, two new terms are generated

$$i\lambda_1 R_1 L_2 + i\lambda_2 L_1 R_2, \quad (2.31)$$

where $i\lambda_1 = 2g_3 \langle L_1 R_2 \rangle$ and $i\lambda_2 = 2g_3 \langle R_1 L_2 \rangle$. The resulting mean-field Hamiltonian is quadratic in the Fermi fields and can again be diagonalized by a Bogoliubov transformation. Let us denote the ground state energy obtained in this way by E_{GS} . The expectation values are determined self-consistently, e.g.

$$-i \langle R_a L_a \rangle = \frac{\partial E_{GS}}{\partial \tilde{\Delta}_a}. \quad (2.32)$$

The SCMF procedure is easily implemented once the appropriate couplings g_a are specified. However, in order to keep matters as simple as possible we will assume from now on that the g_a are small and as a result the differences between the free theory and the SCMF theory are negligible. The main qualitative effect of nonzero g_a is to make the gap of the third Majorana magnetic field dependent. Such a dependence is observed for example in experiments on NDMAP^{4,5} and implies the presence of interactions in the framework of the Majorana fermion model.

D. Decay Processes in the Low-Field Phase

Within the SCMF approximation the role of the current-current interactions is merely to induce slight changes of the dispersion relations of the three coherent single-particle magnon modes. As we will now show, treating the interactions beyond the SCMF approximation leads to the damping of one of the magnons.

The analysis of the spectrum summarized above establishes that there are three different types of magnons, which we will refer to as M_3 , M_+ and M_- respectively. The corresponding dispersion relations are $\omega_3(k)$ (2.12) and $\omega_{\pm}(k)$ (2.20). The interaction of these modes is described by the term \mathcal{H}' in the Hamiltonian (2.1) and involves four particles. As $\omega_-(k)$ can become very small as the magnetic field is increased from zero, the decays $M_3 \rightarrow M_-M_-M_-$ and $M_+ \rightarrow M_-M_-M_-$ become kinematically allowed for sufficiently large magnetic fields. However, the decay of M_3 is forbidden by the symmetry $\mathbf{T}_R\mathbf{R}_{\pi}^z$: M_3 is odd under this symmetry whereas M_{\pm} are even. Essentially we are using the fact that all 3 magnon modes only exist near wave-vector $\frac{\pi}{a_0}$ so that they can only decay into an odd number of magnons. The decay of M_3 into any odd number of M_- 's would be inconsistent with the R_{π}^z spin rotation symmetry. On the other hand the decay $M_+ \rightarrow M_-M_-M_-$ is allowed by symmetry. The process becomes kinematically possible as soon as the magnetic field exceeds a critical value H_d , which is defined by

$$\omega_+(0) = 3\omega_-(0) . \quad (2.33)$$

Solving for H_d we find

$$H_d = \sqrt{\frac{m^2}{4} - \Delta^2} . \quad (2.34)$$

As long as $2\Delta < m$ the decay process will occur for $H > H_d$ and from now on we will assume that this is the case.

We note that in zero field there are no decay processes even if the gaps are such that they are kinematically allowed ($3\Delta_1 < \Delta_2$). The reason is that for $H = 0$ the lattice Hamiltonian (1.1) has additional spin rotational symmetries around the x and y axes by 180 degrees. In combination with the translation symmetry these induce symmetries of the form (2.11) for the Majoranas 1 and 2 individually rather than the combination (2.8). This additional symmetry forbids decay processes.

Inserting the mode expansions (2.16) into the expression for \mathcal{H}' , integrating over the spatial coordinate and then carrying out the Bogoliubov transformation (2.19) generates several terms quartic in the fermionic creation annihilation operators $c_{\pm}(k)$, $c_{\pm}^{\dagger}(k)$. The most interesting one describes the decay of a M_+ mode into three M_- modes and is of the form

$$V = g_3 \int_{-\infty}^{\infty} \frac{dk_1 dk_2 dk_3}{(2\pi)^3} f(k_1, k_2, k_3) \\ \times c_{-}^{\dagger}(k_1) c_{-}^{\dagger}(k_2) c_{-}^{\dagger}(k_3) c_{+}(k_1 + k_2 + k_3) . \quad (2.35)$$

Here f is an antisymmetric function of its arguments and at small momenta is of the form

$$f(k_1, k_2, k_3) \simeq \tilde{C} (k_1 - k_2)(k_1 - k_3)(k_2 - k_3) . \quad (2.36)$$

The constant \tilde{C} is a complicated function of Δ , m and H . The differential rate for the decay of a M_+ particle with momentum p into three M_- particles with momenta p_1, p_2, p_3 is

$$d\Gamma = 2\pi |M|^2 \delta(p - \sum_{j=1}^3 p_j) \delta(\omega_+(p) - \sum_{j=1}^3 \omega_-(p_j)) \\ \times \frac{dp_1 dp_2 dp_3}{3!} , \quad (2.37)$$

where the factor of $3!$ is introduced to account for the fact that the three particles in the final state are indistinguishable. In the Born approximation the transition matrix element M is

$$M = \frac{1}{4\pi^2} \langle 0 | \prod_{j=1}^3 c_{-}(p_j) V c_{+}^{\dagger}(p) | 0 \rangle \left(\delta(p - \sum_{j=1}^3 p_j) \right)^{-1} \\ = \frac{g_3}{2\pi} \frac{3!}{2\pi} f(p_1, p_2, p_3) . \quad (2.38)$$

Taking the M_+ particle to be at rest, i.e. setting $p = 0$, we obtain

$$\Gamma = \frac{6g_3^2}{2\pi} \int dp_1 dp_2 |f(p_1, p_2, -p_1 - p_2)|^2 \\ \times \delta(\omega_+(0) - \omega_-(p_1) - \omega_-(p_2) - \omega_-(p_1 + p_2)) . \quad (2.39)$$

In order to simplify matters further, we concentrate on the case where the magnetic field is close the critical field H_d at which the decay $M_+ \rightarrow M_- M_- M_-$ first becomes kinematically possible. In this regime we have

$$\omega_+(0) - 3\omega_-(0) \ll \omega_-(0) . \quad (2.40)$$

Then the momenta $p_{1,2}$ in (2.39) have to be small in order to satisfy the delta-function and we may use the expansions (2.36) for f and

$$\begin{aligned} \omega_-(p) &\approx \omega_-(0) + \tilde{\alpha}p^2 + \mathcal{O}(p^4) , \\ \tilde{\alpha} &= v^2 \left[1 - \frac{H^2}{m\sqrt{H^2 + \Delta^2}} \right] [2\omega_-(0)]^{-1} . \end{aligned} \quad (2.41)$$

This leads to the following expression for the decay rate in the regime $H > H_d$, $\frac{H}{H_d} - 1 \ll 1$

$$\begin{aligned} \Gamma &\approx \frac{6g_3^2}{2\pi} \frac{\tilde{C}^2}{(2\tilde{\alpha})^4} \frac{4\pi}{\sqrt{3}} [\omega_+(0) - 3\omega_-(0)]^3 \\ &\approx g_3^2 \sqrt{3} \tilde{C}^2 \left[\frac{2}{\tilde{\alpha}} \right]^4 \left[1 - \frac{\Delta^2}{4m^2} \right]^{\frac{3}{2}} (H - H_d)^3 . \end{aligned} \quad (2.42)$$

We find that the decay rate is proportional to $(H - H_d)^3$ and is therefore quite small in the vicinity of H_d .

III. LANDAU-GINZBURG (LG) MODEL

A different approach to studying the spin-1 Heisenberg chain with crystal field anisotropies in a magnetic field was used in Refs [10,14]. It is based on the nonlinear sigma model description of the spin-S Heisenberg chain in terms of the three-component field $\vec{\varphi}$ describing the staggered components of the spin operators and the subsequent approximation of replacing the constraint $\vec{\varphi}^2 = 1$ by a $|\vec{\varphi}|^4$ interaction. The LG Lagrangian density is^{10,14}

$$\begin{aligned} \mathcal{L} &= \frac{1}{2v} \left(\frac{\partial \vec{\varphi}}{\partial t} + \vec{H} \times \vec{\varphi} \right)^2 - \frac{v}{2} \left(\frac{\partial \vec{\varphi}}{\partial x} \right)^2 \\ &\quad - \sum_{a=1}^3 \frac{\Delta_a^2}{2v} \varphi_a^2 - \lambda |\vec{\varphi}|^4 . \end{aligned} \quad (3.1)$$

We again take the magnetic field to point along the 3-axis

$$\vec{H} = H \vec{e}_3 . \quad (3.2)$$

It then follows from (3.1) that φ_3 couples to the magnetic field only via the $\lambda |\vec{\varphi}|^4$ interaction. The Landau-Ginzburg theory inherits the discrete symmetries (1.3) and (1.4) from the underlying lattice model. As is the Majorana fermion model it is convenient to combine the translational symmetry by one site \mathbf{T}_R with the rotation around the z-axis by π \mathbf{R}_π^z and obtain the following two Z_2 symmetries

$$\mathbf{R}_\pi^z : \quad \varphi_a \longrightarrow -\varphi_a , \quad a = 1, 2. \quad (3.3)$$

$$\mathbf{T}_R \mathbf{R}_\pi^z : \quad \varphi_3 \longrightarrow -\varphi_3 . \quad (3.4)$$

The resulting $Z_2 \otimes Z_2$ symmetry is the same as for the Majorana fermion model.

A. Spectrum and Mode Expansion

Neglecting the $|\vec{\varphi}|^4$ interaction the spectrum can be determined by solving the classical equations of motion

$$\left[\frac{\partial^2}{\partial t^2} - v^2 \frac{\partial^2}{\partial x^2} + \Delta_a^2 - H^2 \right] \varphi_a + 2\varepsilon^{abc} H_b \frac{\partial \varphi_c}{\partial t} = 0. \quad (3.5)$$

One finds that there are three magnon modes M_3 and M_{\pm} with the following dispersion relations^{10,14}

$$\begin{aligned}\omega_3(k) &= \sqrt{\Delta_3^2 + v^2 k^2}, \\ \omega_{\pm}(k) &= \left[H^2 + \frac{\Delta_1^2 + \Delta_2^2}{2} + v^2 k^2 \right. \\ &\quad \left. \pm \sqrt{2H^2(\Delta_1^2 + \Delta_2^2 + 2v^2 k^2) + \left(\frac{\Delta_1^2 - \Delta_2^2}{2} \right)^2} \right]^{\frac{1}{2}}.\end{aligned}\quad (3.6)$$

The low energy M_- mode with dispersion $\omega_-(k)$ becomes gapless at a critical field $H_c = \Delta_1$. The resulting critical point is in the universality class of the two-dimensional Ising model¹⁴.

The scalar fields $\varphi_{1,2}$ have the following mode expansions

$$\begin{aligned}\varphi_1(t, x) &= \sum_{\alpha=\pm} \int dk \frac{A_{1\alpha}(k) e^{-i\omega_{\alpha}(k)t + ikx} a_{\alpha}(k) + \text{h.c.}}{\sqrt{4\pi\omega_{\alpha}(k)/v}}, \\ \varphi_2(t, x) &= \sum_{\alpha=\pm} \int dk \frac{iA_{2\alpha}(k) e^{-i\omega_{\alpha}(k)t + ikx} a_{\alpha}(k) + \text{h.c.}}{\sqrt{4\pi\omega_{\alpha}(k)/v}},\end{aligned}\quad (3.7)$$

where $A_{a\alpha}^*(k) = A_{a\alpha}(k)$. Here a and a^\dagger obey canonical commutation relations

$$[a_{\alpha}(k), a_{\beta}^{\dagger}(p)] = \delta_{\alpha\beta} \delta(k - p), \quad (3.8)$$

and the amplitudes $A_{a\pm}(k)$ are fixed by the requirements that (i) the fields φ_a fulfil the equations of motion (3.5) and (ii) the fields φ_a and the conjugate momenta $\Pi_a = \frac{1}{v} \frac{\partial \varphi_a}{\partial t} + (\vec{H} \times \vec{\varphi})_a$ fulfil canonical commutation relations

$$\begin{aligned}[\varphi_a(t, x), \varphi_b(t, y)] &= 0, \quad [\Pi_a(t, x), \Pi_b(t, y)] = 0, \\ [\varphi_a(t, x), \Pi_b(t, y)] &= i\delta_{ab} \delta(x - y).\end{aligned}\quad (3.9)$$

We find

$$\begin{aligned}A_{1+}^2(k) &= \frac{3H^2 + \Delta_1^2 + v^2 k^2 - \omega_-(k)^2}{\omega_+(k)^2 - \omega_-(k)^2}, \\ A_{1-}^2(k) &= 1 - A_{1+}^2(k) = \frac{\omega_+(k)^2 - 3H^2 - \Delta_1^2 - v^2 k^2}{\omega_+(k)^2 - \omega_-(k)^2}, \\ \frac{A_{2a}(k)}{A_{1a}(k)} &= -\frac{\omega_a(k)^2 + H^2 - \Delta_1^2 - v^2 k^2}{2H\omega_a(k)}, \quad a = \pm.\end{aligned}\quad (3.10)$$

Eqns (3.10) allow us to deduce the polarizations of the modes corresponding to the dispersion $\omega_{\pm}(k)$. For example, at $H = 0$ the M_- mode is polarized entirely along the 1 direction and the M_+ mode along the 2 direction. On the other hand, as $H \rightarrow \Delta_1$ we find that

$$\begin{aligned}A_{2-}(0) &\rightarrow 0, \quad A_{2+}(0) \rightarrow 1, \\ A_{1-}^2(0) &\rightarrow \frac{\Delta_2^2 - \Delta_1^2}{3\Delta_1^2 + \Delta_2^2}, \quad A_{1+}^2(0) \rightarrow \frac{4\Delta_1^2}{3\Delta_1^2 + \Delta_2^2}.\end{aligned}\quad (3.11)$$

Hence φ_2 couples only to the M_+ mode whereas φ_1 couples to the M_+ mode as well as to the M_- mode with a strength set by the anisotropy.

B. Decay Processes

In the absence of the nonlinear $|\vec{\varphi}|^4$ -term the LG model describes three coherent magnons M_3 , M_{\pm} with corresponding dispersion relations (3.6). Inclusion of the $|\vec{\varphi}|^4$ term generates interaction terms involving four particles. As was the case in the Majorana fermion model, $\omega_-(k)$ can become very small when the magnetic field is increased and

as a result the decays $M_3 \rightarrow M_-M_-M_-$ and $M_+ \rightarrow M_-M_-M_-$ become kinematically allowed. The decay of M_3 is forbidden by the symmetry $\mathbf{T}_R\mathbf{R}_\pi^z$ (3.4): M_3 is odd under this symmetry whereas M_\pm are even. On the other hand the decay process $M_+ \rightarrow 3M_-$ is allowed when the magnetic field is larger than

$$H_d = \left[\frac{17}{16}[\Delta_1^2 + \Delta_2^2] \pm \frac{5}{16}\sqrt{13[\Delta_1^4 + \Delta_2^4] + 10\Delta_1^2\Delta_2^2} \right]^{\frac{1}{2}}. \quad (3.12)$$

The interaction describing this decay process is given by

$$V = \frac{\lambda v^2}{2\pi} \int_{-\infty}^{\infty} dk_1 dk_2 dk_3 g(k_1, k_2, k_3) \times a_-^\dagger(k_1) a_-^\dagger(k_2) a_-^\dagger(k_3) a_+(k_1 + k_2 + k_3), \quad (3.13)$$

where $g(k_1, k_2, k_3)$ is a symmetric function of its arguments. Its zero momentum limit is

$$g(0, 0, 0) = \frac{A_{1-}(0)^3 A_{1+}(0)}{\sqrt{\omega_-^3 \omega_+}} \left[1 - \left(\frac{\omega_-^2 + H^2 - \Delta_1^2}{2H\omega_-} \right)^2 \right] \left[1 + \frac{\omega_-^2 + H^2 - \Delta_1^2}{2H\omega_-} \frac{\omega_+^2 + H^2 - \Delta_1^2}{2H\omega_+} \right] \equiv \frac{C}{\sqrt{\omega_-^3 \omega_+}}. \quad (3.14)$$

where $\omega_\pm \equiv \omega \pm (0)$. As a first approximation we neglect all interactions except V and calculate the decay rate $M_+ \rightarrow 3M_-$ in the Born approximation.

The differential rate for the decay of a M_+ magnon with momentum p into three M_- magnons with momenta p_1, p_2, p_3 is again given by (2.37), where

$$M = \langle 0 | \prod_{j=1}^3 a_-(p_j) V a_+(p) | 0 \rangle \left(\delta(p - \sum_{j=1}^3 p_j) \right)^{-1} = \frac{3\lambda v^2}{\pi} g(p_1, p_2, p_3). \quad (3.15)$$

Taking the M_+ magnon to be at rest, i.e. setting $p = 0$, we obtain

$$\Gamma = \frac{3\lambda^2 v^4}{\pi} \int dp_1 dp_2 |g(p_1, p_2, -p_1 - p_2)|^2 \times \delta(\omega_+(0) - \omega_-(p_1) - \omega_-(p_2) - \omega_-(p_1 + p_2)). \quad (3.16)$$

For H slightly larger than H_d we again have

$$\omega_+(0) - 3\omega_-(0) \ll \omega_-(0), \quad (3.17)$$

and the momenta $p_{1,2}$ in (3.16) have to be small in order to satisfy the delta-function. We may use the expansions (3.14) for g and

$$\omega_-(p) \approx \omega_-(0) + \alpha p^2 + \mathcal{O}(p^4), \quad \alpha = \frac{v^2}{2\omega_-(0)} \left[1 - \frac{2H^2}{\sqrt{2H^2(\Delta_1^2 + \Delta_2^2) + (\frac{\Delta_1^2 - \Delta_2^2}{2})^2}} \right]. \quad (3.18)$$

This leads to the following expression for the decay rate in the regime $H > H_d$, $\frac{H}{H_d} - 1 \ll 1$

$$\Gamma \approx \frac{\sqrt{3}\lambda^2 v^4 C^2}{\alpha \omega_-(0)^3 \omega_+(0)}. \quad (3.19)$$

The result (3.19) would suggest that the decay rate switches on suddenly at a finite value as soon as H becomes larger than H_d . The underlying reason for this jump is the restricted phase space of a one-dimensional system. The ‘‘free boson’’ result (3.19) for the decay rate is dramatically different from the result obtained in the framework of

the Majorana fermion theory. This poses the question whether (3.19) is robust if we take into account interactions among the magnons in the final state. This amounts to resumming the leading infrared divergences in a perturbative expansion in λ . If we assume that in the low-energy limit the M_- degrees of freedom in the Landau-Ginzburg model can still be mapped onto a Bose gas with δ -function interactions¹⁶, the result of a such a resummation can be determined by exploiting the fact the wave functions of the M_- modes reduce to a free fermion form in the limit of small momenta¹⁹. A three-particle state in the position representation can be written as

$$|\lambda_1, \lambda_2, \lambda_3\rangle = \int dx_1 dx_2 dx_3 \chi(x_1, x_2, x_3) \times a_-^\dagger(x_1) a_-^\dagger(x_2) a_-^\dagger(x_3) |0\rangle, \quad (3.20)$$

where the wave-function is given by

$$\chi_3(x_1, x_2, x_3) = \frac{(-i)^3}{(2\pi)^{3/2} 3!} \prod_{j < k=1}^3 \text{sgn}(x_j - x_k) \times \sum_{P \in S_3} \text{sgn}(P) e^{\sum_{j=1}^3 i\lambda_{P_j} x_j}. \quad (3.21)$$

Here P denotes a permutation of three elements and S_3 the symmetric group of degree 3. In momentum space we have

$$|\lambda_1, \lambda_2, \lambda_3\rangle = \int \frac{dk_1 dk_2 dk_3}{(2\pi)^3} \prod_{j=1}^3 \frac{2k_j}{k_j^2 + \epsilon^2} a_-^\dagger(\lambda_1 - k_2 - k_3) a_-^\dagger(\lambda_2 - k_1 + k_3) a_-^\dagger(\lambda_3 + k_1 + k_2) |0\rangle. \quad (3.22)$$

Taking (3.22) as the final state, the matrix element of the decay vertex is

$$M = \frac{\langle \lambda_3, \lambda_2, \lambda_1 | V a_+^\dagger(p) | 0 \rangle}{\delta(p - \sum_{j=1}^3 \lambda_j)} = \frac{3\lambda v^2}{\pi} \int \prod_{j=1}^3 \frac{dq_j}{2\pi} \frac{2q_j}{q_j^2 + \epsilon^2} g(\lambda_1 - q_2 - q_3, \lambda_2 - q_1 + q_3, \lambda_3 + q_1 + q_2). \quad (3.23)$$

It follows from the definition (3.23) that the matrix element is an antisymmetric function of $\lambda_1, \lambda_2, \lambda_3$. As long as we are interested in the decay rate for H close to H_d , we may expand M for small λ_j . The leading term antisymmetric in $\lambda_{1,2,3}$ is then

$$C'(\lambda_1 - \lambda_2)(\lambda_1 - \lambda_3)(\lambda_2 - \lambda_3), \quad (3.24)$$

For small λ_j the matrix element is thus equal to

$$M = \frac{3\lambda C' v^2}{\pi} \prod_{j < k} (\lambda_j - \lambda_k). \quad (3.25)$$

Following through the same steps as before, the decay rate for H close to H_d with the M_+ magnon initially at rest is found to be

$$\Gamma \approx \frac{\sqrt{3}\lambda^2 C'^2 v^4}{4\alpha^4} [\omega_+(0) - 3\omega_-(0)]^3 \propto [H - H_d]^3. \quad (3.26)$$

Comparing the decay rate (3.26) to the result (3.19) we see that interactions in the final state have a dramatic effect: rather than turning on at a finite value as soon as H exceeds H_d , the decay rate (3.26) actually vanishes at H_d and exhibits the same power law behavior for $H > H_d$ as the decay rate in the Majorana fermion model. This may suggest that the dependence of the decay rate on $H - H_d$ is a robust result that holds for the underlying lattice model as well.

IV. VICINITY OF THE ISING CRITICAL POINT

As we have seen above, both the Majorana fermion model and the Landau-Ginzburg theory lead to an Ising critical point at some values H_c of the applied magnetic field. In the simplest approximations where interactions are neglected,

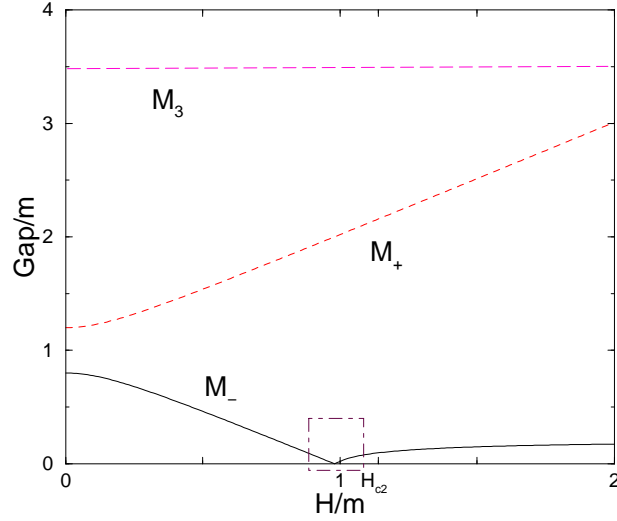


FIG. 1: Magnon gaps as functions of the applied field for the Majorana fermion model with $g_a = 0$. The gaps in zero field are chosen as $\Delta_1 = 0.8m$, $\Delta_2 = 1.2m$ and $\Delta_3 = 3.5m$. The square indicates the window in energies and fields in which the description in terms of an effective Ising model is appropriate.

the actual values for H_c are rather different, but as we are interested only in robust features this numerical difference does not really concern us here. More importantly both theories predict that the low-energy behaviour in the vicinity of the critical point is described by an off-critical Ising model with Hamiltonian

$$\mathcal{H} = \frac{iv}{2} [L\partial_x L - R\partial_x R] - im_0 RL . \quad (4.1)$$

Here the mass parameter that parametrizes the deviation from criticality is equal to the smallest magnon gap

$$|m_0| \simeq \omega_-(k=0, H) . \quad (4.2)$$

The description by (4.1) is appropriate at low energies $\omega \ll \min\{\omega_+(k=0, H), \omega_3(k=0, H)\}$ and H sufficiently smaller than the critical field H_{c2} (2.22) at which incommensurabilities develop. The Hamiltonian (4.1) exhibits a Z_2 symmetry

$$R \longrightarrow -R , \quad L \longrightarrow -L , \quad (4.3)$$

under which the Ising order (σ) and disorder (μ) parameters transform as

$$\begin{aligned} \underline{H < H_c} : \quad & \sigma \longrightarrow -\sigma , \\ & \mu \longrightarrow \mu , \\ \underline{H > H_c} : \quad & \sigma \longrightarrow \sigma , \\ & \mu \longrightarrow -\mu . \end{aligned} \quad (4.4)$$

In order to determine the magnetic low-energy response (in the vicinity of the antiferromagnetic wave number) we need to express the staggered magnetizations n^a in terms of operators related to the Ising model (4.1). As was pointed out in Ref.[14], the dominant contribution to the staggered magnetization in the x -direction should be the Ising order parameter field

$$n^x = \mathcal{C}_x(H) \sigma + \dots \quad (4.5)$$

Here $\mathcal{C}_x(H)$ is an unknown constant and the dots indicate contributions from less relevant operators. The underlying reason for the identification (4.5) is simply that in the ordered phase of the Ising model (which corresponds to $H > H_c$) one has a nonzero expectation value $\langle \sigma \rangle \neq 0$, whereas in the disordered phase (which occurs at $H < H_c$) one has $\langle \sigma \rangle = 0$. The staggered magnetization in both the Majorana fermion and LG models exhibits the same kind of behaviour and it is then natural to expect the identification (4.5). In Appendix D we present arguments that suggest that the staggered magnetization along the y -direction has the following low-energy projection

$$n^y = \mathcal{C}_y(H) \partial_\tau \sigma + \dots \quad (4.6)$$

In what follows we chose a short-distance normalization for the field σ in the theory (4.1) such that for $\tau^2 + x^2/v^2 \rightarrow 0$

$$\langle \sigma(\tau, x) \sigma(0, 0) \rangle \longrightarrow \frac{1}{[\tau^2 + x^2/v^2]^{1/8}}. \quad (4.7)$$

We will use the integrability of the theory (4.1) to determine the dynamical structure factor $S^{\text{xx}}(\omega, \frac{\pi}{a_0} + q)$ at low energies, where the staggered component of S^x is given by (4.5). The yy component then follows from (4.6)

$$S^{\text{yy}}(\omega, \frac{\pi}{a_0} + q) \propto \frac{\omega^2}{m^2} S^{\text{xx}}(\omega, \frac{\pi}{a_0} + q). \quad (4.8)$$

1. $H < H_c$: Low-Field Phase

By the Z_2 symmetry (4.3),(4.4) only intermediate states with an odd number of magnons contribute to the two-point correlation functions of the Ising order parameter field σ and hence the staggered structure factor $S^{\text{xx}}(\omega, \frac{\pi}{a_0} + q)$ at low energies. The leading contributions are²⁰⁻²³

$$\begin{aligned} S^{\text{xx}}(\omega, \frac{\pi}{a_0} + q) &= \frac{vA}{\sqrt{m_0^2 + v^2 q^2}} \delta\left(\omega - \sqrt{m_0^2 + v^2 q^2}\right) \\ &+ \frac{2vA}{3\pi^2 m_0^2} \int_0^{z_0} dz \frac{(\tanh(z) \tanh(\frac{y+z}{2}) \tanh(\frac{y-z}{2}))^2}{\sqrt{[x^2 - 1 - 4 \cosh^2 z]^2 - 16 \cosh^2 z}} \\ &+ \text{contributions from } 5, 7, \dots \text{ magnons,} \end{aligned} \quad (4.9)$$

where

$$A = C_x^2(H) 2^{\frac{1}{6}} e^{-\frac{1}{4}} \mathcal{A}^3 m_0^{\frac{1}{4}}, \quad (4.10)$$

$$x^2 = \frac{\omega^2 - v^2 q^2}{m_0^2},$$

$$z_0 = \text{arccosh}\left(\frac{x-1}{2}\right),$$

$$y = \text{arccosh}\left(\frac{x^2 - 1 - 4 \cosh^2 z}{4 \cosh z}\right). \quad (4.11)$$

Here

$$A = 1.28242712910062\dots \quad (4.12)$$

is Glaisher's constant. The three-magnon contribution is always very small. In the frequency interval $[0, 30m_0]$ roughly 100 times more spectral weight sits in the single-magnon contribution than in the three-particle one. Hence the magnetic response below energies of the order of tens of the magnon gap m_0 is dominated by the coherent magnon contribution. However, if H becomes very close to H_c the magnon gaps m_0 tends to zero. If we are interested in the magnetic response at a low (compared to the gap of the second coherent magnon mode) but fixed energy we have to take the contributions of intermediate states with 5, 7, 9, ... magnons into account in order to get an accurate result for $S^{\text{xx}}(\omega, \frac{\pi}{a_0} + q)$.

2. $H = H_c$: At Criticality

At criticality the structure factor exhibits a power-law behaviour²⁴

$$S^{\text{xx}}(\omega, \frac{\pi}{a_0} + q) = \text{Im} \left\{ \mathcal{B} [v^2 q^2 - (\omega + i\varepsilon)^2]^{-\frac{7}{8}} \right\}, \quad (4.13)$$

where

$$\mathcal{B} = 2v C_x^2(H) 2^{\frac{3}{4}} \frac{\Gamma(\frac{7}{8})}{\Gamma(\frac{1}{8})}. \quad (4.14)$$

3. $H > H_c$: High-field Phase

In this phase there is a nonzero staggered magnetization and correspondingly a nonzero expectation value for the Ising order parameter

$$\langle \sigma \rangle \neq 0, \quad (4.15)$$

which results in a Bragg peak for momentum transfer $\frac{\pi}{a_0}$ along the chain direction. By virtue of the Z_2 symmetry (4.4) only intermediate states with an even number of magnons contribute to $S^{\text{xx}}(\omega, \frac{\pi}{a_0} + q)$. The leading contribution to the inelastic neutron scattering cross section comes from intermediate states involving *two* magnons²⁰⁻²², which leads to the following result

$$S^{\text{xx}}(\omega, \frac{\pi}{a_0} + q) = \frac{vA}{\pi} \frac{\sqrt{s^2 - 4m_0^2}}{s^3} \theta(s - 2m_0) \\ + \text{contributions from 4, 6, } \dots \text{ magnons.} \quad (4.16)$$

Here A is given by (4.10) and $s^2 = \omega^2 - v^2 q^2$.

V. THE HIGH-FIELD PHASE FOR WEAK ANISOTROPY

In general it is difficult to determine the effects of magnon-interactions in quantitative detail. An exception is the case of a small anisotropy of the zero-field gaps

$$\Delta \ll m, \quad (5.1)$$

where $2m = \Delta_1 + \Delta_2$ and $\Delta = \Delta_2 - \Delta_1$. As we will show, if the magnetic field is sufficiently larger than the critical field H_c and

$$\Delta \ll H - H_c \lesssim J, \quad (5.2)$$

it is possible to determine the interaction effects on the magnetic response at low energies in some detail. More precisely, we consider magnetic fields sufficiently larger than the field H_{c2} (see e.g. (2.22)), at which incommensurabilities begin to develop. The scale defining the low-energy region is the difference Δ . As is shown in Appendix E, the low-energy effective Hamiltonian is given by a sine-Gordon model (SGM)¹⁴

$$\mathcal{H} = \frac{\tilde{v}}{16\pi} [(\partial_x \Theta)^2 + (\partial_x \Phi)^2] - 2\mu \cos \beta \Theta. \quad (5.3)$$

Here \tilde{v} is the spin velocity, $\mu \propto \Delta$ and β is a function of the applied magnetic field H . The high-energy cutoff of the theory (5.3) is $H - H_c$. At low energies the dominant Fourier component of the transverse spin operators is at $q = \frac{\pi}{a_0}$

$$S_j^\pm \longrightarrow (-1)^j A \exp\left(\pm \frac{i\beta}{2} \Theta\right). \quad (5.4)$$

The identification (5.4) is in accordance with the fact that in the high-field phase there is Néel order along the x-direction

$$\langle (-1)^n S_n^x \rangle \propto \langle \cos\left(\frac{\beta}{2} \Theta\right) \rangle \neq 0. \quad (5.5)$$

We choose a short-distance normalization such that for $|x - y| \rightarrow 0$

$$e^{i\alpha\Theta(x)} e^{i\gamma\Theta(y)} \longrightarrow |x - y|^{4\alpha\gamma} e^{i\alpha\Theta(x) + i\gamma\Theta(y)}. \quad (5.6)$$

The amplitude A in (5.4) is nonuniversal and not known in general. However, very close to H_c

$$\Delta \ll H - H_c \ll H_c, \quad (5.7)$$

it is given by (see Appendix F)

$$A = A' \left[\frac{a_0^4 m}{v^2} (H - H_c) \right]^{\frac{1}{8}}, \quad (5.8)$$

where A' is a field independent numerical constant. The dependence of (5.8) on $H - H_c$ is a *universal feature of the C-IC transition*.

We note that the sign of the cos-term in (5.3) is quite important. Flipping the sign corresponds to a shift $\Theta \rightarrow \Theta + \pi/\beta$, which essentially leads to an exchange of the x and y component of the spin operators in (5.4).

The value of the parameter β is of crucial importance. For the isotropic case ($\Delta_2 = \Delta_1$) it has recently been determined¹³ in the framework of the nonlinear sigma model description of the spin-S Heisenberg chain. In the isotropic case the high-field phase at $H > H_c$ is a Luttinger liquid and β is related to the Luttinger liquid parameter. It was found that¹³

$$\beta = \frac{1}{\sqrt{2}S_R(\theta_F)}, \quad (5.9)$$

where $S_R(\theta)$ fulfils the integral equation

$$S_R(\theta) = 1 + \int_{-\theta_F}^{\theta_F} d\theta' S_R(\theta') \frac{1}{\pi^2 + (\theta - \theta')^2}. \quad (5.10)$$

Here θ_F is determined as a function of the magnetic field H by

$$\begin{aligned} \epsilon(\theta) &= m \cosh(\theta) - H + \int_{-\theta_F}^{\theta_F} d\theta' \epsilon(\theta') \frac{1}{\pi^2 + (\theta - \theta')^2}, \\ \epsilon(\theta_F) &= 0. \end{aligned} \quad (5.11)$$

Similarly one may determine the spin velocity

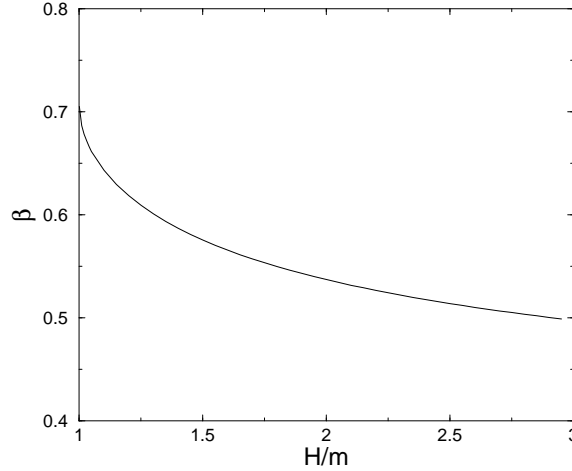


FIG. 2: Parameter β as function of the applied magnetic field.

$$\tilde{v} = \frac{v}{2\pi\rho(\theta)} \left. \frac{\partial\epsilon(\theta)}{\partial\theta} \right|_{\theta=\theta_F}, \quad (5.12)$$

where $\rho(\theta)$ fulfils the integral equation

$$\rho(\theta) = \frac{m}{2\pi} \cosh(\theta) + \int_{-\theta_F}^{\theta_F} d\theta' \rho(\theta') \frac{1}{\pi^2 + (\theta - \theta')^2}. \quad (5.13)$$

The parameter β as well as the velocity \tilde{v} entering the sine-Gordon Hamiltonian (5.3) may be estimated with a good degree of accuracy from their respective values in the isotropic case as long as $\frac{\Delta_2 - \Delta_1}{\Delta_2} \ll 1$. On the other hand, the agreement between the Luttinger liquid parameter calculated in the nonlinear sigma model and the one of the isotropic spin-1 Heisenberg chain in a magnetic field, which is known approximately from DMRG computations¹⁷, was shown to be fairly good in Ref.[13]. Hence we may determine β with a reasonable degree of accuracy from (5.9) as long as $\frac{\Delta_2 - \Delta_1}{\Delta_2} \ll 1$. It then follows that $\beta < \frac{1}{\sqrt{2}}$ and hence the SGM (5.3) is in the attractive regime.

A. Spectrum of the SGM

The SGM (5.3) is integrable and many exact results are available. The spectrum of the SGM depends on the value of the coupling constant β . In the so-called repulsive regime, $1/\sqrt{2} < \beta < 1$, there are only two elementary excitations, called soliton and antisoliton. These have a massive relativistic dispersion,

$$E(P) = \sqrt{M^2 + \tilde{v}^2 P^2}, \quad (5.14)$$

where M is the gap.

In the regime $0 < \beta < 1/\sqrt{2}$ relevant to our discussion, soliton and antisoliton attract and can form bound states, known as “breathers”. There are

$$\mathcal{N} = \left[\frac{1 - \beta^2}{\beta^2} \right] \quad (5.15)$$

different types of breathers, where $[x]$ in (5.15) denotes the integer part of x . The breather gaps are given by

$$M_n = 2M \sin(n\pi\xi/2), \quad n = 1, \dots, \mathcal{N}, \quad (5.16)$$

where

$$\xi = \frac{\beta^2}{1 - \beta^2}. \quad (5.17)$$

The number of breathers is a function of the applied magnetic field H . There always is at least one breather. A second breather appears above a field H_0 , which is determined by the requirement

$$\beta = \frac{1}{\sqrt{3}}. \quad (5.18)$$

This requirement is fulfilled for

$$H > H_0 \approx 1.5M. \quad (5.19)$$

B. Dynamical Structure Factor

A basis of eigenstates of the SGM is given by scattering states of solitons, antisolitons and breathers. In order to distinguish these we introduce labels $B_1, B_2, \dots, B_{\mathcal{N}}, s, \bar{s}$. As usual for particles with relativistic dispersion, it is useful to introduce a rapidity variable θ to parameterize energy and momentum

$$E_s(\theta) = M \cosh \theta, \quad P_s(\theta) = (M/\tilde{v}) \sinh \theta, \quad (5.20)$$

$$E_{\bar{s}}(\theta) = M \cosh \theta, \quad P_{\bar{s}}(\theta) = (M/\tilde{v}) \sinh \theta, \quad (5.21)$$

$$E_{B_n}(\theta) = M_n \cosh \theta, \quad P_{B_n}(\theta) = (M_n/\tilde{v}) \sinh \theta. \quad (5.22)$$

Two-point functions are expressed in terms of a basis of scattering states of solitons, antisolitons and breathers as summarized in Appendix B, see Eqn (B8). After carrying out the double Fourier transform we arrive at the following representation for the imaginary part of the retarded two-point function of the operator \mathcal{O} for $\omega > 0$

$$S^{\mathcal{O}}(\omega, q) = \sum_{n=1}^{\infty} \sum_{\epsilon_i} \int \frac{d\theta_1 \dots d\theta_n}{(2\pi)^{n-1} n!} |f_{\epsilon_1 \dots \epsilon_n}^{\mathcal{O}}(\theta_1 \dots \theta_n)|^2 \delta(q - \sum_j M_{\epsilon_j} \sinh \theta_j / \tilde{v}) \delta(\omega - \sum_j M_{\epsilon_j} \cosh \theta_j) \quad (5.23)$$

The form factors of the operators $\exp(\pm i\beta\Phi/2)$ in the sine-Gordon model were determined in Ref. [28,29]. Using these results we can determine the first few terms of the expansion (5.23) for the transverse spin operators. We have

$$S^{\text{xx}}(\omega, \frac{\pi}{a_0} + q) = C \left\{ \pi f_2 \delta(s^2 - M_2^2) \Theta(H - H_0) \right.$$

$$\begin{aligned}
S^{\text{yy}}(\omega, \frac{\pi}{a_0} + q) = C \left\{ \right. & \left. + \text{Re} \frac{|F^{\text{cos}}(\theta_0)|^2}{s\sqrt{s^2 - 4M^2}} + \dots \right\}, \\
& \left\{ \begin{aligned} & \pi f_1 \delta(s^2 - M_1^2) \\ & + \text{Re} \frac{|F^{\text{sin}}(\theta_0)|^2}{s\sqrt{s^2 - 4M^2}} + \dots \end{aligned} \right\}. \tag{5.24}
\end{aligned}$$

Here C is an overall (dimensionful) constant. The terms proportional to F^{sin} and F^{cos} represent the contributions by intermediate states involving one soliton and one antisoliton and

$$\theta_0 = 2\text{arccosh}(s/2M). \tag{5.25}$$

The δ -function contributions are due to the breather bound states. The soliton-antisoliton form factors are given by^{28,29}

$$\begin{aligned}
|F^{\text{sin}}(\theta)|^2 &= \left| \langle 0 | \sin\left(\frac{\beta}{2}\Phi(0)\right) |\theta_2\theta_1\rangle_{+-} \right|^2 \\
&= \left| \frac{g(\theta)}{\xi \cosh\left(\frac{\theta+i\pi}{2\xi}\right)} \right|^2, \\
|F^{\text{cos}}(\theta)|^2 &= \left| \langle 0 | \cos\left(\frac{\beta}{2}\Phi(0)\right) |\theta_2\theta_1\rangle_{+-} \right|^2 \\
&= \left| \frac{g(\theta)}{\xi \sinh\left(\frac{\theta+i\pi}{2\xi}\right)} \right|^2, \tag{5.26}
\end{aligned}$$

where $\theta = \theta_2 - \theta_1$ and

$$\begin{aligned}
g(\theta) &= i \sinh \theta / 2 \\
&\times \exp\left(\int_0^\infty \frac{dt \sinh^2(t[1 - i\theta/\pi]) \sinh(t[\xi - 1])}{t \sinh 2t \sinh \xi t \cosh t}\right). \tag{5.27}
\end{aligned}$$

The absolute values squared of the breather form factors are^{28,29}

$$\begin{aligned}
f_1 &= 2 \sin\left(\frac{\pi\xi}{2}\right) \exp\left(-2 \int_0^{\pi\xi} \frac{dt}{2\pi} \frac{t}{\sin t}\right), \\
f_2 &= \frac{2|g(-i\pi[1 - 2\xi])|^2}{\cot(\pi\xi) \cot(\frac{\pi\xi}{2})^2}. \tag{5.28}
\end{aligned}$$

An important result is that the first bound state B_1 is visible only in S^{yy} and does not couple to S^{xx} . We note that there are additional contributions in the spectral representations (5.24) at higher energies. For example, there is a two-breather B_1B_1 contribution to S^{xx} at energies above $2M_1$.

We plot $S^{\alpha\alpha}(\omega, \frac{\pi}{a_0})$ as functions of ω/M for several values of the applied magnetic field in Figs 3-4. In order to give a visual impression of their spectral weights we have broadened the δ -functions corresponding to the breathers by convolution with a Gaussian.

We first discuss the evolution of $S^{\text{yy}}(\omega, \frac{\pi}{a_0})$ shown in Fig. 3: as H moves away from $H_c = m$ the breather B_1 splits off from the soliton-antisoliton continuum and very quickly takes over most of the spectral weight. Except for a narrow window (in magnetic field) above H_c the yy-component of the dynamical structure factor is dominated by a *coherent* single-particle peak.

The evolution of $S^{\text{xx}}(\omega, \frac{\pi}{a_0})$ is very different as is shown in Fig. 4: as H moves away from $H_c = m$ the incoherent soliton-antisoliton continuum slowly narrows (on the scale of the field-dependent soliton gap) until it eventually begets the second, heavy breather B_2 at $H = H_0 \approx 1.5m$. Over a large interval of magnetic fields $S^{\text{xx}}(\omega, \frac{\pi}{a_0})$ is dominated by the *incoherent* soliton-antisoliton continuum.

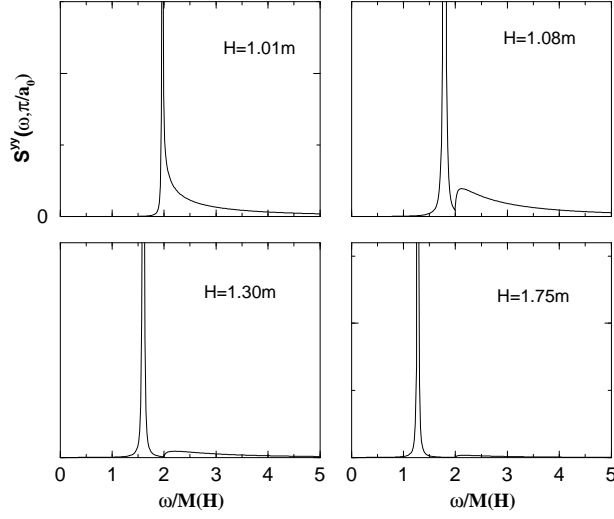


FIG. 3: $S^{yy}(\omega, \frac{\pi}{a_0})$ as a function of ω/M for several values of the applied field H .

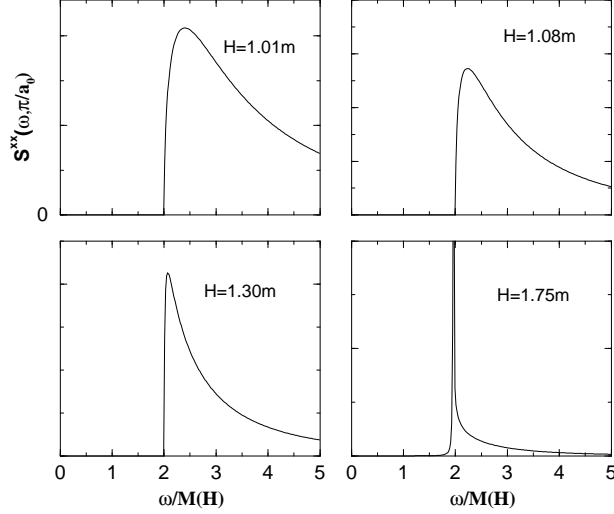


FIG. 4: $S^{xx}(\omega, \frac{\pi}{a_0})$ as a function of ω/M for several values of the applied field H .

1. Spectral Weights

In order to compare the spectral weights located in the coherent breather peaks to the spectral weight associated with the soliton-antisoliton continua it is useful to define quantities

$$\begin{aligned}
 I^{xx} &= \frac{M^2}{C} \int_0^{25} dx S^{xx}(xM, \frac{\pi}{a_0}) \equiv I_{B_2}^{xx} + I_{ss}^{xx}, \\
 I^{yy} &= \frac{M^2}{C} \int_0^{25} dx S^{yy}(xM, \frac{\pi}{a_0}) \equiv I_{B_1}^{yy} + I_{ss}^{yy}.
 \end{aligned}
 \tag{5.29}$$

For example, CI^{yy}/M^2 is the spectral weight of the yy-component of the dynamical structure factor at the antiferromagnetic wave number integrated over the frequency interval $[0, 25M]$. It has contributions $I_{B_1}^{yy}$ from the coherent breather peak and I_{ss}^{yy} from the soliton antisoliton continuum (there are also contributions due to B_1B_2 two-breather states *etc*, but their contributions are subleading). It is important to note that the soliton gap M and the overall factor C depend on the applied magnetic field. These dependencies drop out once we consider spectral weight ratios

such as

$$\frac{I_{ss}^{yy}}{I_{B_1}^{yy}}, \quad \frac{I_{ss}^{xx}}{I_{B_1}^{yy}}, \quad \frac{I_{B_2}^{xx}}{I_{B_1}^{yy}}. \quad (5.30)$$

These ratios are plotted as functions of β in Fig.5. We see that for small β (that is at $H \gg H_c$) most of the spectral weight is situated in the coherent peak associated with the first breather B_1 . Very close to the transition the second breather does not exist and most of the spectral weight sits in the soliton-antisoliton continua. The crossover between these two regimes occurs around $\beta \approx 0.675$, which according to Fig. 2 corresponds to

$$\frac{H}{H_c} \approx 1.025. \quad (5.31)$$

The lesson is that interactions make the summed dynamical structure factor

$$S^{xx}(\omega, \frac{\pi}{a_0} + q) + S^{yy}(\omega, \frac{\pi}{a_0} + q) \quad (5.32)$$

look coherent expect for fields very close to H_c . On the other hand, the polarized structure factor $S^{xx}(\omega, \frac{\pi}{a_0} + q)$ looks incoherent! It would be very interesting to attempt to disentangle the components of the dynamical structure factor in inelastic neutron scattering experiments and in this way observe this incoherent scattering continuum.

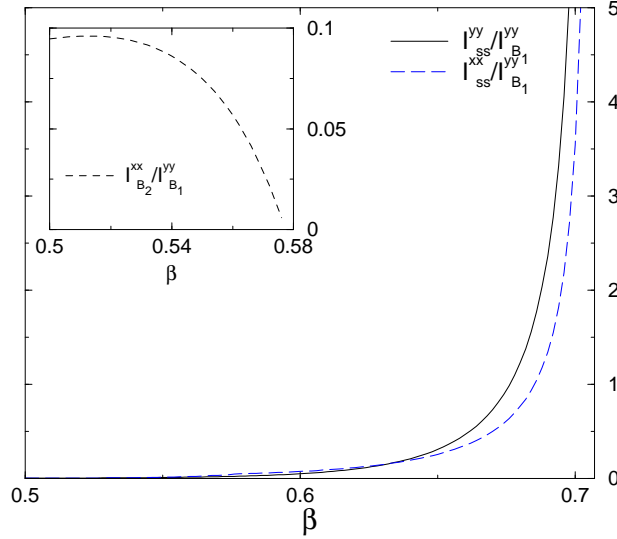


FIG. 5: Spectral weight ratios $I_{ss}^{yy}/I_{B_1}^{yy}$, $I_{ss}^{xx}/I_{B_1}^{yy}$ and $I_{B_2}^{xx}/I_{B_1}^{yy}$ as functions of the parameter β .

2. Polarizations in the LG model

How do these results fit into the general picture of the LG model? In the latter one expands to quadratic order in the fields φ_1 and φ_2 around the minimum of the effective potential at $\vec{\varphi}_{\text{vac}} = (m_0, 0, 0)$

$$m_0^2 = \frac{H^2 - \Delta_1^2}{4v\lambda}. \quad (5.33)$$

The effective Lagrangian for the fields $\varphi_{1,2}$ becomes

$$\begin{aligned} \mathcal{L} = & \sum_{a=1}^2 \frac{1}{2v} \left(\frac{\partial \varphi_a}{\partial t} \right)^2 - \frac{v}{2} \left(\frac{\partial \varphi_a}{\partial x} \right)^2 - \frac{H_c}{v} \epsilon_{abc} \frac{\partial \varphi_a}{\partial t} \varphi_b \\ & - \frac{H^2 - \Delta_1^2}{v} \varphi_1^2 - \frac{\Delta_2^2 - \Delta_1^2}{2v} \varphi_2^2. \end{aligned} \quad (5.34)$$

This is the same as (3.1) for the fields $\varphi_{1,2}$ if we make the replacement (in (3.1))

$$\begin{aligned}\Delta_1^2 &\longrightarrow 3H^2 - 2\Delta_1^2, \\ \Delta_2^2 &\longrightarrow \Delta_2^2 + H^2 - \Delta_1^2.\end{aligned}\tag{5.35}$$

This implies for the polarizations in the limit $H \gg \Delta_2$

$$\frac{A_{2-}(0)}{A_{1-}(0)} \longrightarrow - \left[\frac{3H^2}{\Delta_2^2 - \Delta_1^2} \right]^{\frac{1}{2}}.\tag{5.36}$$

In other words

$$|A_{2-}| \gg |A_{1-}|,\tag{5.37}$$

and as a result the coherent low-energy mode is dominantly polarized along the y-direction! This agrees nicely with the sine-Gordon calculation, where the dominant feature, the first breather, appears in S^{vy} .

VI. INTERCHAIN COUPLING

So far we have considered a purely one-dimensional situation corresponding to an ensemble of uncoupled spin-1 chains. As long as the magnon gap is large, a weak coupling between the chains may be neglected in a first approximation. On the other hand, the interchain exchange is expected to lead to significant qualitative changes in the magnetic response close to the critical point where the magnon gap becomes very small³⁵. In order to assess the effects of a weak interchain coupling for $H \approx H_c$ we consider a Landau-Ginzburg model of the form

$$\mathcal{L} = \sum_n \mathcal{L}_n + \mathcal{L}_{\text{int}},\tag{6.1}$$

where

$$\begin{aligned}\mathcal{L}_n &= \frac{1}{2v} \left(\frac{\partial \vec{\varphi}_n}{\partial t} + \vec{H} \times \vec{\varphi}_n \right)^2 - \frac{v}{2} \left(\frac{\partial \vec{\varphi}_n}{\partial x} \right)^2 \\ &\quad - \sum_{a=1}^3 \frac{\Delta_a^2}{2v} \varphi_{n,a}^2 - \lambda |\vec{\varphi}_n|^4, \\ \mathcal{L}_{\text{int}} &= \frac{J_{\perp}}{a_0} \sum_{\langle j,k \rangle} \vec{\varphi}_j \cdot \vec{\varphi}_k.\end{aligned}\tag{6.2}$$

Here the sum $\langle jk \rangle$ is over links between neighbouring sites on different chains and we have dropped quartic terms in \mathcal{L}_{int} that arise from the interaction of the smooth components of the spin operators.

As we have seen in section IV, close to the the Ising critical point the low-energy degrees of freedom are described by off-critical Ising models. Hence at low energies we have

$$\mathcal{L}_n \approx R_n \partial_- R_n + L_n \partial_+ L_n - im_0 R_n L_n.\tag{6.3}$$

The leading low-energy projection of the interchain exchange follows from (4.5), (4.6)

$$\mathcal{L}_{\text{int}} \approx \frac{J_{\perp}}{a_0} C^2 \left[\frac{a_0}{v} \right]^{1/4} \sum_{\langle j,k \rangle} \sigma_j \sigma_k,\tag{6.4}$$

where C is a dimensionless constant. The ‘‘quasi-1D Ising model’’ (6.3), (6.4) has recently been studied in Ref. [36] and we may follow some of this analysis here.

A. Mean-Field Approximation

As a first step, we analyze the model (6.3), (6.4) by means of a self-consistent mean-field approximation^{30,31}. We assume the existence of a nonzero expectation value

$$\langle \sigma \rangle \neq 0,\tag{6.5}$$

which corresponds to Néel order along the x-direction. The long-range order can be induced by the magnetic field, the interchain coupling or by both. In the presence on a nonzero expectation value (6.5) we may decouple the interaction term in (6.4) and arrive at the following mean-field Lagrangian density

$$\mathcal{L}_{\text{MF}} = R\partial_- R + L\partial_+ L - im_0 RL + \frac{h}{v} \sigma . \quad (6.6)$$

Here “magnetic field” h has dimensions of $s^{-\frac{15}{8}}$ by virtue of the normalization (4.7) and is subject to the self-consistency condition

$$h = \mathcal{Z} C^2 v \frac{J_{\perp}}{a_0} \left[\frac{a_0}{v} \right]^{\frac{1}{4}} \langle \sigma \rangle , \quad (6.7)$$

where \mathcal{Z} is the number of neighbouring chains. The mean-field theory is purely one-dimensional and describes an off-critical Ising model in an effective magnetic field induced by the neighbouring chains. The model (6.6) has been studied by several authors^{32–34} and is known to exhibit very interesting physical behaviour as m_0 and h are varied. In order to discuss the effects of h and m_0 it is convenient to consider the Euclidean two-point function of Ising order parameters

$$\chi_{\sigma\sigma}^E(\bar{\omega}, q) = \int_{-\infty}^{\infty} dx d\tau e^{i\bar{\omega}\tau - iqx} \langle \sigma(\tau, x) \sigma(0, 0) \rangle . \quad (6.8)$$

We note that $\chi_{\sigma\sigma}^E$ is related to the xx-component of the staggered susceptibility by analytic continuation to real frequencies. The Lagrangian (6.6) defines a one-parameter family of field theories labelled by the dimensionless quantity³⁴

$$\chi = m_0 h^{-\frac{8}{15}} . \quad (6.9)$$

In the two special cases $\chi = 0$ and $|\chi| = \infty$ the model(6.6) is integrable and the susceptibility (6.8) can be determined to a very high accuracy by means of the formfactor bootstrap approach. In what follows we first review known quantitative results for the cases $|\chi| \rightarrow \infty$ and $\chi \rightarrow 0$ and then summarize the qualitative behaviour for general values of χ .

1. The Limit $h \rightarrow 0$: McCoy-Wu Scenario

The regime $h \rightarrow 0$ was studied in Refs^{32,33} by means of a perturbative expansion in h . In the absence of a field ($h = 0$) the dynamical structure factor has been given in section IV. For $m_0 > 0$ the Ising model is in its disordered phase and the spin-spin correlation functions are dominated by a single-particle pole and the next-lowest excited states occur in the form of a three-particle scattering continuum. The dynamical structure factor is proportional to (4.9). Introducing a small magnetic field leads to a small shift in the position of the single-particle pole. Furthermore a two-particle scattering continuum of excited states emerges.

For $m_0 < 0$ the Ising model is in its ordered phase. This means that there is a nonzero value for the staggered magnetization

$$\langle \sigma \rangle_0^2 = 2^{1/6} e^{-1/4} A^3 m_0^{1/4} , \quad (6.10)$$

where A denotes Glaisher’s constant (4.12). The structure factor in the ordered phase is given by (4.16): the structure factor is incoherent and there is a two-particle branch cut starting at $\omega = 2m_0$.

It is convenient to define a dimensionless magnetic field \tilde{h} by

$$\tilde{h} = \frac{\langle \sigma \rangle_0}{m_0^2} h . \quad (6.11)$$

After a resummation of a perturbative expansion in \tilde{h} McCoy and Wu established that the spin-spin correlation function has the following large-distance behaviour³²

$$\begin{aligned} \langle \sigma(\tau, x) \sigma(0, 0) \rangle &\approx \langle \sigma \rangle_0^2 \frac{\exp(-2m_0 r)}{2\sqrt{\pi m_0 r}} \tilde{h} \\ &\times \sum_l \exp(-m_0 r (\lambda_l \tilde{h})^{2/3}) , \end{aligned} \quad (6.12)$$

where $r^2 = \tau^2 + x^2/v^2$ and λ_l are the positive solutions to the equation

$$J_{\frac{1}{3}}(\lambda_l/3) + J_{-\frac{1}{3}}(\lambda_l/3) = 0 . \quad (6.13)$$

The interesting point is that the Fourier transform of (6.12) no longer has a branch cut! There are single-particle poles at

$$\bar{\omega}^2 + v^2 q^2 = -[2 + (\tilde{h}\lambda_l)^{2/3}]^2 m_0^2 . \quad (6.14)$$

In other words, the two-particle branch cut has disintegrated into a series of single-particle poles. The residues of these poles are proportional to

$$\tilde{h} [2 + (\tilde{h}\lambda_l)^{2/3}]^{-1} . \quad (6.15)$$

Hence the lightest particle carries more spectral weight than the heavier ones. This is quite different from the result for $h = 0$ where the structure factor vanishes as the threshold is approached from above.

2. The Limit $m_0 \rightarrow 0$: Magnetic Deformation

In the limit $m_0 \rightarrow 0$ the model (6.6) is integrable³⁷. The spectrum consists of eight types of massive self-conjugate particles. Three of them have masses below the lowest two-particle threshold. The two-point function of the Ising order operator σ was calculated by the form factor bootstrap approach in Ref.[38]. The dominant contribution to the two point function of Ising order parameter fields is due to the lightest particles. The dynamical susceptibility is approximately

$$\chi_{\sigma\sigma}(\omega, q) \approx \left[\frac{4m_1^2}{15\pi h} \right]^2 \sum_{j=1}^3 \frac{2vZ_j}{\omega^2 - v^2q^2 - m_j^2} , \quad (6.16)$$

where the particle masses are^{37,43}

$$\begin{aligned} m_1 &\approx 4.40490858 h^{\frac{8}{15}} , \\ m_2 &\approx 1.618 m_1 , \quad m_3 \approx 1.989 m_1 . \end{aligned} \quad (6.17)$$

and^{36,38}

$$Z_1 \approx 0.247159 , \quad Z_2 \approx 0.069017 , \quad Z_3 \approx 0.02096 , \quad (6.18)$$

The expectation value of the Ising order parameter is⁴³

$$\langle \sigma \rangle \approx 1.07496 h^{\frac{1}{15}} , \quad (6.19)$$

which enables us in principle to solve the self-consistency equation (6.7). The important point is that most of the spectral weight is located in the coherent modes corresponding to the two lightest particles. The ratio of weights between them is

$$\frac{(Z_1/m_1)}{(Z_2/m_2)} \approx 5.79427 . \quad (6.20)$$

The region $m_0 \approx 0$ limit was studied by form factor perturbation theory in Ref.[34].

3. Qualitative Behaviour in the general case

For general values of χ the qualitative behaviour of $\chi_{\sigma\sigma}^E(\bar{\omega}, q)$ is known and may be conveniently summarized^{32,34} by considering the evolution of $\chi_{\sigma\sigma}^E$ with χ along a path in the $m_0 - h$ plane as shown in Fig. 6.

In Fig.7 we show the analytic structure of $\chi_{\sigma\sigma}^E$ as a function of $s = \sqrt{\bar{\omega}^2 + v^2q^2}$ for various locations along the path set out in Fig.6. For example, point (a) corresponds to the disordered phase of the off-critical Ising model, where in Euclidean space there is a single-particle pole at $s = im_0$ and a 3-particle branch cut along the positive imaginary axis starting at $s = 3im_0$. Point (b) shows the small shift in the position of the pole and the emergence of a 2-particle

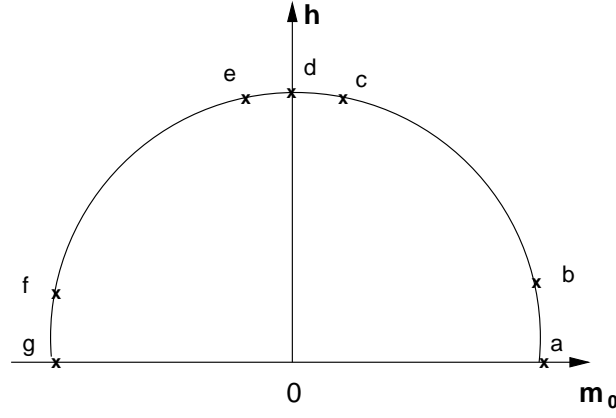


FIG. 6: Path in the $h - m_0$ plane of the transverse Ising model in a magnetic field.

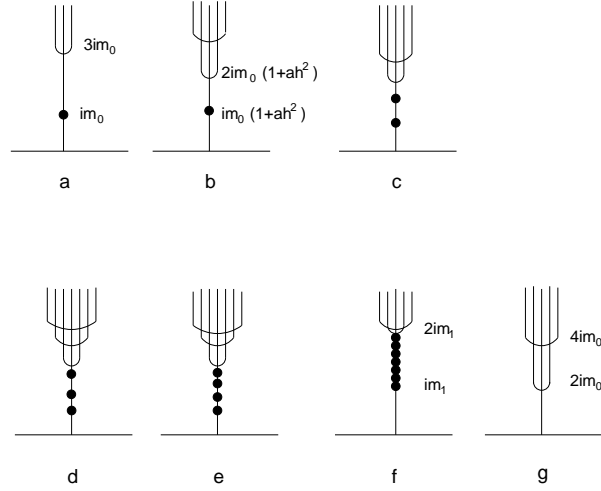


FIG. 7: Structure of poles and branch cuts of $\chi_{\sigma\sigma}^E(\bar{\omega}, q)$ at the points (a)-(g) in the $h - m_0$ plane indicated in Fig.6 ($m_1 = m_0[2 + (\tilde{h}\lambda_1)^{\frac{2}{3}}]$).

branchcut³². Points (c)-(e) describe the vicinity of the Ising model in a magnetic field; there are several single-particle poles below a 2-particle branchcut and the number of these poles increases as we move along the path. Finally, points (f)-(g) describe the breakup of the 2-particle branchcut mentioned above.

An important point is that for $m_0 < 0$, which corresponds to the ordered phase of the Ising model for $h = 0$, the general effect of the magnetic field is to make the dynamical susceptibility look more coherent in these sense that the low-energy regime is dominated by single-particle poles. In particular, a weak interchain coupling in the ordered phase close to H_c leads to a disintegration of the 2-particle scattering continuum that dominates the dynamical structure factor (4.16) and the formation of a series of single-particle poles.

B. Beyond Mean-Field: RPA

It is straightforward to go beyond the mean-field approximation by resumming all diagrams in the interchain coupling that do not involve loops. This leads to the RPA expression for the dynamical susceptibility³⁹

$$\chi^{xx}(\omega, q, \mathbf{k}) = \frac{\chi^{xx}(\omega, q)}{1 - 2J_{\perp}(\mathbf{k})\chi^{xx}(\omega, q)}, \quad (6.21)$$

where $J_{\perp}(\mathbf{k})$ is the Fourier transform of the interchain coupling and

$$\chi^{xx}(\omega, q) = \frac{C^2}{a_0} \left[\frac{a_0}{v} \right]^{\frac{1}{4}} \chi_{\sigma\sigma}(\omega, q). \quad (6.22)$$

In our notations

$$J_{\perp}(\mathbf{k}) = J_{\perp}[\cos(k_y a_0) + \cos(k_z a_0)] \quad (6.23)$$

for a simple cubic lattice. It was shown in Ref.[36] that in the vicinity of points (c)-(e) of Fig.6 the RPA leads only to slight changes of the mean-field results. More precisely, single-particle excitations corresponding to poles at $s = m$ (with residue $Z/2m$) in the 1D susceptibility $\chi^{xx}(\omega, q)$ acquire a transverse dispersion $ZJ_{\perp}(\mathbf{k})$ in the RPA.

VII. SUMMARY AND DISCUSSION

We have studied the spectrum and dynamical spin correlations for Haldane-gap systems in the presence of a magnetic field. We have paid particular attention to the role played by the crystal field anisotropies present in materials like NDMAP. We have concentrated on the case where the magnetic field is applied along the same same direction as the largest single-ion anisotropy D (which we identify with the z-direction in spin space). Generalizations of our results to other cases is straightforward. Our main results are as follows:

- At low fields there are three coherent modes M_{-} , M_{+} , M_3 . Their respective gaps $\Delta_{-}(H) < \Delta_{+}(H) < \Delta_3(H)$ are field-dependent.
- Above a critical field H_d , M_2 develops a finite lifetime via the decay process $M_{+} \rightarrow M_{-}M_{-}M_{-}$. M_{-} and M_3 retain infinite lifetimes.
- At a critical field $H_c > H_d$ the gap $\Delta_{-}(H)$ vanishes. In the vicinity of H_c the low energy degrees of freedom are described by an (off-critical) Ising model and the dynamical structure factor is calculated by exact methods. For $H > H_c$ the dynamical structure factor is dominated by an incoherent two-particle scattering continuum above a finite-energy threshold.
- At fields sufficiently above H_c the low-energy degrees of freedom are described by a sine-Gordon model. $S^{yy}(\omega, \frac{\pi}{a_0} + q)$ is dominated by a coherent single-particle bound state with a spectral gap below a two-particle scattering continuum. The most pronounced feature in $S^{xx}(\omega, \frac{\pi}{a_0} + q)$ is an incoherent two-particle scattering continuum above a finite-energy threshold.
- The effects of interchain coupling are most pronounced in the vicinity of H_c . Taking it into account in a mean-field fashion leads to a purely one-dimensional effective description at low energies in terms of an *Ising model in a magnetic field*. This suggests that Haldane-gap materials with single-ion anisotropies in a magnetic field may constitute a realization of this very interesting theory. Within the mean-field description the main effect of interchain coupling is to generate coherent single-particle modes from the incoherent scattering continua. As a result the dynamical structure factor will appear more “coherent”.

Our findings shed some light on the question why recent inelastic neutron scattering experiments on NDMAP^{4,5} have failed to find any evidence of scattering continua in the high-field phase. At large fields these are suppressed through bound-state formation, whereas in the vicinity of the critical field H_c the coupling between chains effects similar shifts of spectral weight to single-particle modes. It would be interesting to investigate some of our predictions experimentally. In particular we hope that it may be possible to

1. address the issue of the finite lifetime of M_2 above the critical field H_d .
2. disentangle the xx and yy components of the structure factor at high fields. According to our predictions the xx-component will remain incoherent up to fairly large fields so that a scattering continuum may be observable.

Acknowledgments

We thank R.M. Konik, A.A. Nersesyan, S. Shapiro, A.M. Tsvelik, I. Zaliznyak and A. Zheludev for important discussions. We acknowledge support by the U.S. Department of Energy under Contract No DE-AC02-98 CH10886 (FE), the EPSRC under grant GR/R83712/01 (FE), the Theory Institute for Strongly Correlated and Complex Systems at BNL (IA), where much of this research was carried out, the Canadian Institute for Advanced Research (IA) and NSERC of Canada (IA).

APPENDIX A: LOW-FIELD PHASE IN THE ABSENCE OF CRYSTAL FIELD ANISOTROPY

In the absence of a crystal field anisotropy the Hamiltonian is

$$\mathcal{H}(h) = J \sum_n \mathbf{S}_n \cdot \mathbf{S}_{n+1} - h S^z. \quad (\text{A1})$$

The Heisenberg equations of motion read

$$\begin{aligned} \frac{d}{dt} S_n^\pm(t) &= i[\mathcal{H}(0), S_n^\pm] \mp ih S_n^\pm, \\ \frac{d}{dt} S_n^z(t) &= i[\mathcal{H}(0), S_n^z]. \end{aligned} \quad (\text{A2})$$

Equations (A2) permit us to express the dynamical susceptibilities for $h \neq 0$ in terms of the ones in zero field

$$\begin{aligned} \chi^{+-}(\omega, q, h) &= \chi^{+-}(\omega - h, q, 0), \\ \chi^{-+}(\omega, q, h) &= \chi^{-+}(\omega + h, q, 0), \\ \chi^{zz}(\omega, q, h) &= \chi^{zz}(\omega, q, 0). \end{aligned} \quad (\text{A3})$$

This implies is that the structure factors in a field are simply the same as in zero field apart from constant shifts in energy. The leading contributions to the dynamical susceptibilities in zero field have been calculated in the framework of the O(3) nonlinear-sigma model approximation to the isotropic spin-1 Heisenberg chain in Refs [23,41]. It follows from these results that the three-particle contributions are very small. We note that the threshold of the $M_+M_+M_-$ three-particle continuum (two $S^z = 1$ magnons and one $S^z = -1$ magnon) is at $3\Delta - h$, i.e. for any $H < H_c$ it still is very slightly higher in energy than the highest energy M_- magnon mode. Hence all three magnon modes remain “sharp” for all $H < H_c$.

We note that analogous considerations apply in the presence of a single-ion anisotropy in z-direction only ($E = 0$ in (1.1) and a magnetic field along the z-direction). The dynamical susceptibilities for finite fields can then be expressed in terms of the zero field susceptibilities through the equation of motions for the spin operators. This is quite useful for the Majorana fermion model, where the staggered components of the spin operators are expressed in terms of Ising order and disorder operators. The latter transform nontrivially under the Bogoliubov transformation used to diagonalize the Hamiltonian for nonzero magnetic fields.

APPENDIX B: SPECTRAL REPRESENTATION OF CORRELATION FUNCTIONS

In this appendix we collect useful formulas for spectral representations of correlation functions in massive, integrable, relativistic quantum field theories.

We parametrize energy and momentum of single particle states in terms of a rapidity variable θ

$$E_\epsilon(\theta) = \Delta_\epsilon \cosh \theta, \quad P_\epsilon(\theta) = \frac{\Delta_\epsilon}{v} \sinh \theta. \quad (\text{B1})$$

Here the index ϵ labels the different types of particles and Δ_ϵ are the corresponding spectral gaps. A scattering state of N particles with rapidities $\{\theta_j\}$ and indices $\{\epsilon_j\}$ is denoted by

$$|\theta_1, \theta_2, \dots, \theta_N\rangle_{\epsilon_1, \epsilon_2, \dots, \epsilon_N}. \quad (\text{B2})$$

Its energy and momentum are

$$E(\{\theta_j\}) = \sum_{j=1}^N \Delta_{\epsilon_j} \cosh \theta_j, \quad P(\{\theta_j\}) = \sum_{j=1}^N \frac{\Delta_{\epsilon_j}}{v} \sinh \theta_j. \quad (\text{B3})$$

A basis of states is most easily constructed in terms of the generators of the so-called Faddeev-Zamolodchikov algebra

$$\begin{aligned} Z^{\epsilon_1}(\theta_1) Z^{\epsilon_2}(\theta_2) &= \mathbf{S}_{\epsilon_1', \epsilon_2'}^{\epsilon_1, \epsilon_2}(\theta_1 - \theta_2) Z^{\epsilon_2'}(\theta_2) Z^{\epsilon_1'}(\theta_1), \\ Z_{\epsilon_1}^\dagger(\theta_1) Z_{\epsilon_2}^\dagger(\theta_2) &= Z_{\epsilon_2'}^\dagger(\theta_2) Z_{\epsilon_1'}^\dagger(\theta_1) \mathbf{S}_{\epsilon_1, \epsilon_2}^{\epsilon_1', \epsilon_2'}(\theta_1 - \theta_2), \\ Z^{\epsilon_1}(\theta_1) Z_{\epsilon_2}^\dagger(\theta_2) &= Z_{\epsilon_2'}^\dagger(\theta_2) \mathbf{S}_{\epsilon_2, \epsilon_1'}^{\epsilon_1, \epsilon_2'}(\theta_2 - \theta_1) Z^{\epsilon_1'}(\theta_1) \\ &\quad + 2\pi \delta_{\epsilon_2}^{\epsilon_1} \delta(\theta_1 - \theta_2). \end{aligned} \quad (\text{B4})$$

Here $\mathbf{S}_{\epsilon'_1, \epsilon'_2}^{\epsilon_1, \epsilon_2}(\theta)$ is the factorizable two-particle scattering matrix of the integrable quantum field theory. Using the ZF operators a Fock space of states can be constructed as follows. The vacuum is defined by

$$Z_{\epsilon_i}(\theta)|0\rangle = 0. \quad (\text{B5})$$

Multiparticle states are then obtained by acting with strings of creation operators $Z_{\epsilon}^{\dagger}(\theta)$ on the vacuum

$$|\theta_n \dots \theta_1\rangle_{\epsilon_n \dots \epsilon_1} = Z_{\epsilon_n}^{\dagger}(\theta_n) \dots Z_{\epsilon_1}^{\dagger}(\theta_1)|0\rangle. \quad (\text{B6})$$

The resolution of the identity in the normalization implied by (B4) is given by

$$1 = \sum_{n=0}^{\infty} \frac{1}{n!} \sum_{\{\epsilon_j\}} \int_{-\infty}^{\infty} \prod_{j=1}^n \frac{d\theta_j}{2\pi} |\theta_n, \dots, \theta_1\rangle_{\epsilon_n, \dots, \epsilon_1} {}^{\epsilon_1, \dots, \epsilon_n} \langle \theta_1, \dots, \theta_n|. \quad (\text{B7})$$

The two point function of some operator \mathcal{O} can now be expressed in the spectral representation as

$$\langle \mathcal{O}^{\dagger}(t, x) \mathcal{O}(0, 0) \rangle = \sum_{n=0}^{\infty} \frac{1}{n!} \sum_{\epsilon_j} \int_{-\infty}^{\infty} \prod_{j=1}^n \frac{d\theta_j}{2\pi} |f_{\epsilon_1 \dots \epsilon_n}^{\mathcal{O}}(\theta_1, \dots, \theta_n)|^2 \exp(-itE(\{\theta_j\}) + ixP(\{\theta_j\})), \quad (\text{B8})$$

where the formfactors are given by

$$f_{\epsilon_1 \dots \epsilon_n}^{\mathcal{O}}(\theta_1 \dots \theta_n) \equiv \langle 0 | \mathcal{O}(0, 0) | \theta_n \dots \theta_1 \rangle_{\epsilon_n \dots \epsilon_1}. \quad (\text{B9})$$

APPENDIX C: BOUND STATES IN THE MAJORANA MODEL

In this appendix we address the question of whether the current-current interaction in the Majorana model leads to the formation of bound states. For simplicity we consider only the SU(2) symmetric case with Hamiltonian

$$\begin{aligned} \mathcal{H} &= \frac{i}{2} \int dx \sum_{a=1}^3 v [L_a \partial_x L_a - R_a \partial_x R_a] - 2m R_a L_a \\ &+ g \int dx \sum_a J^a J^a. \end{aligned} \quad (\text{C1})$$

We aim to establish that bound states exist for any $g > 0$, whereas there are no bound states for $g < 0$. We recall that the Majorana fermion model arises from the spin-Heisenberg Hamiltonian with an additional biquadratic term

$$H_{\text{biquad}} = J \sum_n \mathbf{S}_n \cdot \mathbf{S}_{n+1} - b (\mathbf{S}_n \cdot \mathbf{S}_{n+1})^2, \quad (\text{C2})$$

where $|b - 1| \ll 1$. For $b > 1$ the model is in a dimerized phase whereas $b < 1$ corresponds to a Haldane spin-liquid regime. One may establish by using the expressions (2.5) for the spin operators that the case $b < 1$ ($b > 1$) corresponds to $g < 0$ ($g > 0$). In order to determine whether the current-current interaction leads to the formation of bound states, we first consider the limit of a very anisotropic interaction

$$\begin{aligned} \mathcal{H}_{\text{ani}} &= \frac{i}{2} \int dx \sum_{a=1}^3 v [L_a \partial_x L_a - R_a \partial_x R_a] - 2m R_a L_a \\ &+ g \int dx J^3 J^3. \end{aligned} \quad (\text{C3})$$

This case can be mapped onto a single massive Majorana fermion plus the massive Thirring model by introducing complex Fermi fields by

$$\begin{aligned} R_1 &= \frac{\Psi_R + \Psi_R^{\dagger}}{\sqrt{2}}, & R_2 &= \frac{\Psi_R - \Psi_R^{\dagger}}{i\sqrt{2}}, \\ L_1 &= \frac{\Psi_L^{\dagger} - \Psi_L}{i\sqrt{2}}, & L_2 &= \frac{\Psi_L + \Psi_L^{\dagger}}{\sqrt{2}}. \end{aligned} \quad (\text{C4})$$

The Hamiltonian density is rewritten as $\mathcal{H}_{\text{ani}} = \mathcal{H}_{\text{Maj}} + \mathcal{H}_{\text{MTM}}$, where

$$\begin{aligned}\mathcal{H}_{\text{Maj}} &= \frac{iv}{2} \int dx [L_3 \partial_x L_3 - R_3 \partial_x R_3 - \frac{2m}{v} R_3 L_3], \\ \mathcal{H}_{\text{MTM}} &= -iv \int dx [\Psi_R^\dagger \partial_x \Psi_R - \Psi_L^\dagger \partial_x \Psi_L] \\ &\quad + \int dx [m[\Psi_R^\dagger \Psi_L + \text{h.c.}] + 2g \Psi_L^\dagger \Psi_L \Psi_R^\dagger \Psi_R].\end{aligned}\tag{C5}$$

In Eqn (C5) we have dropped a term proportional to $\int dx [\Psi_R^\dagger \Psi_R + \Psi_L^\dagger \Psi_L]$ as it commutes with the Hamiltonian. It is well known that in the massive Thirring model there are breather bound states for $g > 0$, but no bound states exist for $g < 0$, see e.g. Refs[44].

A different approach is to use large- N methods. If we consider N species of Majorana fermions rather than three, we may decouple the interaction through a bosonic Hubbard-Stratonovich field σ . For even N and $g > 0$ the problems maps onto the $O(N/2)$ massive Gross-Neveu model, which is known to have bosonic bound states in the large- N limit⁴⁵.

APPENDIX D: LOW-ENERGY PROJECTIONS OF THE STAGGERED MAGNETIZATIONS

In this appendix we give arguments in favour of the identification (4.6) at low energies and in the vicinity of the Ising critical point at $H = H_c$. We first consider the LG theory and then the Majorana fermion model.

1. Landau-Ginzburg Model

It is instructive to examine the evolution of the amplitudes $A_{a\alpha}$ entering the mode expansions (3.7) of the scalar fields φ_a as the magnetic field is increased. We recall that the critical field is $H_c = \Delta_1$. In the vicinity of H_c we parametrize

$$H = \Delta_1 - \delta, \quad \delta > 0.\tag{D1}$$

As we are interested only in low energies we may restrict our attention to the “ $-$ ” modes. From (3.10) we obtain the following expansions in δ

$$\begin{aligned}(\omega_{-}(0))^2 &\approx \frac{2\Delta_1(\Delta_2^2 - \Delta_1^2)}{3\Delta_1^2 + \Delta_2^2} \delta, \\ \left[\frac{A_{2-}(0)}{A_{1-}(0)}\right]^2 &= \frac{(7\Delta_1^2 + \Delta_2^2)\delta}{2\Delta_1(3\Delta_1^2 + \Delta_2^2)}.\end{aligned}\tag{D2}$$

Eqns (D2) imply that close to H_c we have

$$A_{2-}(0) \propto \omega_{-}(0) A_{1-}(0).\tag{D3}$$

As we have seen before, close to H_c the x-component of the staggered magnetization φ_1 couples to M_- with a finite amplitude $A_{1-}(0)$ given by (3.11). Furthermore we have the identification (4.6)

$$\varphi_1 \propto \sigma,\tag{D4}$$

where σ is the Ising order parameter field. Eqns (D3) and (D4) together suggest that

$$\varphi_2 \propto \partial_t \sigma.\tag{D5}$$

This claim may be substantiated further in the limit where one of the zero field gaps is much smaller than the other, i.e. $\Delta_1 \ll \Delta_2$. As we are interested in energies that are small compared to Δ_2 , we may “integrate out” the high-energy degrees of freedom corresponding to φ_2 in the path integral expression for the staggered magnetization n^y .

Because $H_c = \Delta_1$ is small, we furthermore may take the magnetic field into account perturbatively. The staggered magnetization in y direction is

$$n^y(t, x) = \varphi_2(t, x) . \quad (\text{D6})$$

Averaging $n^y(t, x)$ over φ_2 , we obtain

$$\begin{aligned} \langle n^y(t, x) \rangle_2 &= \frac{1}{Z} \int \mathcal{D}\varphi_2 \varphi_2(t, x) \\ &\quad \times e^{iS_2 - 2i(H/v) \int dt_1 dx_1 [\varphi_2 \partial_{t_1} \varphi_1]} , \end{aligned} \quad (\text{D7})$$

where

$$S_2 = \int dt dx \left[\frac{1}{2v} (\partial_t \varphi_2)^2 - \frac{v}{2} (\partial_x \varphi_2)^2 - \frac{\Delta_2^2}{2v} \varphi_2^2 \right] . \quad (\text{D8})$$

The leading contribution occurs in first order in the magnetic field

$$\begin{aligned} &\langle n^y(t, x) \rangle_2 \\ &\approx -\frac{2iH}{v} \int dx_1 dt_1 \langle T \varphi_2(t, x) \varphi_2(t_1, x_1) \rangle_2 \partial_t \varphi_1(t_1, x_1) \\ &= \frac{2H}{v} \int dx_1 dt_1 G_2(t - t_1, x - x_1) \partial_t \varphi_1(t_1, x_1) \\ &\approx \frac{2H}{v} \left[\int dx'_1 dt'_1 G_2(t'_1, x'_1) \right] \partial_t \varphi_1(t, x) . \end{aligned} \quad (\text{D9})$$

In the last line we have used that the leading contribution to the integral comes from the region $t_1 \approx t$, $x_1 \approx x$. This shows that the mixing induced by the magnetic field generates a contribution to $n^y(t, x)$ proportional to $\partial_t \varphi_1(t, x)$ at low energies.

2. Majorana Fermion Model

Analogous calculations can be performed in the framework of the Majorana fermion model in the case $g_a = 0$, i.e. in the absence of the current-current interactions. In particular, let us consider the case where one of the zero field gaps is much smaller than the other

$$\Delta_1 \ll \Delta_2 . \quad (\text{D10})$$

As the critical field $H_c = \sqrt{\Delta_1 \Delta_2}$ is much smaller than Δ_2 we may treat the magnetic field term perturbatively. We may derive an effective action for R_1, L_1 only by integrating out R_2 and L_2 (we recall that the third Majorana decouples in the absence of interactions)

$$\begin{aligned} S_{\text{eff}} &\approx S_1 - \frac{1}{2} \langle S_H^2 \rangle_2 , \\ S_H &= iH \int dx d\tau [L_1 L_2 + R_1 R_2] , \end{aligned} \quad (\text{D11})$$

where $\langle \rangle_2$ denotes the expectation value with respect to the second Majorana fermion and

$$\begin{aligned} S_1 &= \int d\tau dx [R_1 \partial_- R_1 + L_1 \partial_+ L_1 - i\Delta_1 R_1 L_1] , \\ \partial_{\pm} &= \frac{\partial_{\tau} \pm iv \partial_x}{2} . \end{aligned} \quad (\text{D12})$$

The Matsubara Green's functions are defined as e.g.

$$G_{RR}(\tau, x) = -\langle T_{\tau} R(\tau, x) R(0) \rangle . \quad (\text{D13})$$

Their Fourier transforms are

$$\begin{aligned}
G_{R_2 R_2}(\omega, q) &= -\frac{i\omega + vq}{\omega^2 + v^2 q^2 + \Delta_2^2}, \\
G_{L_2 L_2}(\omega, q) &= -\frac{i\omega - vq}{\omega^2 + v^2 q^2 + \Delta_2^2}, \\
G_{R_2 L_2}(\omega, q) &= +\frac{i\Delta_2}{\omega^2 + v^2 q^2 + \Delta_2^2}.
\end{aligned} \tag{D14}$$

A straightforward calculation then gives

$$\mathcal{L}_{\text{eff}} = R_1 \partial_- R_1 + L_1 \partial_+ L_1 - i[\Delta_1 - \frac{H^2}{\Delta_2}] R_1 L_1. \tag{D15}$$

In other words, integrating out the second Majorana leads to a renormalization of the mass of the first Majorana. We note that the dispersion relation that follows from (D15) agrees with the expansion of $\omega_-(q)$ (2.20) in the case $H \ll \Delta_2$ as it must. What we have shown is that in the case $\Delta_1 \ll \Delta_2$ it is simply the first Majorana that becomes critical at H_c . The staggered magnetization in x -direction is expressed at low energies by averaging (2.6) with respect to the second and third Majoranas, which gives

$$n^x(x) \propto \sigma^1(x) \langle \mu^2(x) \rangle \langle \mu^3(x) \rangle. \tag{D16}$$

The determination of the operator content of $n^y(x)$ at low energies is significantly more involved. In order to obtain the low-energy projection, we need to average with respect to the second and third Majoranas

$$\begin{aligned}
n^y(0, 0) &\approx -iH \langle \mu_3 \rangle \\
&\times \int d\tau dx \left\{ \langle L_2(\tau, x) \sigma_2(0) \rangle_2 L_1(\tau, x) \mu_1(0) \right. \\
&\quad \left. + \langle R_2(\tau, x) \sigma_2(0) \rangle_2 R_1(\tau, x) \mu_1(0) \right\}.
\end{aligned} \tag{D17}$$

The expectation values $\langle \rangle_2$ with respect to the second Majorana can be evaluated by the form factor bootstrap approach by utilizing the results of Refs[20–22]. We obtain

$$\begin{aligned}
\langle L_2(\tau, x) \sigma_2(0) \rangle_2 &\approx D e^{i\pi/4} \frac{1}{\sqrt{v\tau + ix}} e^{-mr}, \\
\langle R_2(\tau, x) \sigma_2(0) \rangle_2 &\approx D e^{-i\pi/4} \frac{1}{\sqrt{v\tau - ix}} e^{-mr},
\end{aligned} \tag{D18}$$

where $D = m^{1/8} (4\pi)^{-1/2} 2^{1/12} e^{-1/8} A^{3/2}$ and $r^2 = \tau^2 + x^2/v^2$. Using these results in (D17) we see that the integral is dominated with exponential accuracy by the region $\tau \approx 0$, $x \approx 0$. Hence the operator content of n^y is determined by the fusion of the disorder operator μ_1 with the left and right moving fermions L_1, R_1 . The relevant operator product expansions can be worked out following Ref.[46]

$$\begin{aligned}
L(\tau, x) \mu(0) &\approx \frac{\gamma}{\sqrt{z}} \sigma(0) - \frac{m\gamma}{v} \sqrt{\bar{z}} \sigma(0) + \frac{4\gamma}{v} \sqrt{\bar{z}} \partial_- \sigma(0), \\
R(\tau, x) \mu(0) &\approx \frac{\bar{\gamma}}{\sqrt{\bar{z}}} \sigma(0) - \frac{m\bar{\gamma}}{v} \sqrt{z} \sigma(0) + \frac{4\bar{\gamma}}{v} \sqrt{z} \partial_+ \sigma(0),
\end{aligned} \tag{D19}$$

where $z = v\tau + ix$, $\gamma = \exp(-i\pi/4)/\sqrt{4\pi}$ and $\partial_{\mp} = \frac{1}{2}(\partial_{\tau} \mp iv\partial_x)$. Combining (D18) with (D19) we obtain the desired result

$$n^y \propto \partial_{\tau} \sigma. \tag{D20}$$

APPENDIX E: DERIVATION OF THE SINE-GORDON MODEL IN THE HIGH-FIELD PHASE FOR WEAK ANISOTROPY

In this appendix we show how the Sine-Gordon Hamiltonian emerges as the low-energy effective theory at $H > H_c$ in the small anisotropy limit $\Delta_2 - \Delta_1 \ll H - H_c$. We first present a derivation in the framework of the nonlinear sigma model and then within the Majorana fermion model.

1. Nonlinear sigma model

The isotropic spin-S Heisenberg chain in a magnetic field can be mapped onto the O(3) nonlinear sigma model in the continuum limit. Exploiting the integrability of the nonlinear sigma model it was shown in Ref. [13] that for $H > \Delta$ the low-energy regime is described in terms of a free boson

$$\mathcal{H} = \frac{\tilde{v}}{16\pi} \int dx [(\partial_x \Phi)^2 + (\partial_x \Theta)^2]. \quad (\text{E1})$$

Here Θ is the field dual to Φ and fulfils

$$\tilde{v} \partial_x \Theta = -i \partial_\tau \Phi, \quad \partial_\tau \Theta = i \tilde{v} \partial_x \Phi. \quad (\text{E2})$$

The low-energy behaviour of spin correlations follows from the correspondence

$$S_n^\pm \simeq (-1)^n A \exp(\pm i \frac{\beta}{2} \Theta). \quad (\text{E3})$$

The parameters \tilde{v} and β were calculated in Ref. [13]. Adding a very small crystal field anisotropy to the Hamiltonian

$$E \sum_j [(S_j^x)^2 - (S_j^y)^2], \quad (\text{E4})$$

generates a term proportional to

$$\int dx \cos(\beta \Theta). \quad (\text{E5})$$

The resulting theory is the sine-Gordon model (5.3). The term $D \sum_j (S_j^z)^2$ merely leads to a small change in β which we ignore here.

2. Majorana fermion model

Our starting point is the Hamiltonian (2.14) describing the two Majorana fermions that couple to the magnetic field in the limit $\Delta_2 = \Delta_1 = m$, i.e. vanishing gap anisotropy $\Delta = 0$. Using

$$\Psi_{R,L} = \int_{-\infty}^{\infty} \frac{dk}{2\pi} e^{ikx} c_{R,L}(k), \quad (\text{E6})$$

we may express the Hamiltonian as

$$\mathcal{H}_{12} \Big|_{\Delta=0} = \int_{-\infty}^{\infty} \frac{dk}{2\pi} (c_R^\dagger, c_L^\dagger) M \begin{pmatrix} c_R \\ c_L \end{pmatrix} \quad (\text{E7})$$

where

$$M = \begin{pmatrix} vk + H & -im \\ im & -vk + H \end{pmatrix}. \quad (\text{E8})$$

Now we may carry out a Bogoliubov transformation

$$\begin{pmatrix} a_k \\ b_k \end{pmatrix} = \begin{pmatrix} \cos(\varphi_k) & -i \sin(\varphi_k) \\ -i \sin(\varphi_k) & \cos(\varphi_k) \end{pmatrix} \begin{pmatrix} c_R(k) \\ c_L(k) \end{pmatrix} \quad (\text{E9})$$

with

$$\tan(2\varphi_k) = \frac{m}{vk} \quad (\text{E10})$$

to diagonalize the Hamiltonian. We find

$$\mathcal{H}_{12} \Big|_{\Delta=0} = \int \frac{dk}{2\pi} \left[(H + \text{sgn}(k) \sqrt{m^2 + v^2 k^2}) a_k^\dagger a_k + (H - \text{sgn}(k) \sqrt{m^2 + v^2 k^2}) b_k^\dagger b_k \right]. \quad (\text{E11})$$

Introducing fermions c and d by

$$\begin{aligned} c(k) &= a_k \theta(k) + b_k \theta(-k) , \\ d(k) &= b_k \theta(k) + a_k \theta(-k) , \end{aligned} \quad (\text{E12})$$

we may express the Hamiltonian (E11) as

$$\begin{aligned} \mathcal{H}_{12} \Big|_{\Delta=0} &= \int \frac{dk}{2\pi} \left[(H + \sqrt{m^2 + v^2 k^2}) c^\dagger(k) c(k) \right. \\ &\quad \left. + (H - \sqrt{m^2 + v^2 k^2}) d^\dagger(k) d(k) \right]. \end{aligned} \quad (\text{E13})$$

The low-energy modes occur in the lower band in the vicinity of $\pm k_F = \pm \sqrt{(H^2 - m^2)/v^2}$. They can be combined into left and right moving Fermi fields by

$$d(x) = \exp(-ik_F x) R(x) + \exp(ik_F x) L(x) . \quad (\text{E14})$$

The low-energy effective Hamiltonian is then

$$\mathcal{H}' = i\tilde{v} \int dx [L^\dagger \partial_x L - R^\dagger \partial_x R] , \quad (\text{E15})$$

where $\tilde{v} = v^2 k_F / H$. We now bosonize the low-energy Hamiltonian using

$$\begin{aligned} R^\dagger(x) &\sim \frac{1}{\sqrt{2\pi}} \exp\left(i \frac{\Phi(x) + \Theta(x)}{2\sqrt{2}}\right) , \\ L^\dagger(x) &\sim \frac{1}{\sqrt{2\pi}} \exp\left(-i \frac{\Phi(x) - \Theta(x)}{2\sqrt{2}}\right) . \end{aligned} \quad (\text{E16})$$

Here φ and $\bar{\varphi}$ are chiral Bose fields fulfilling the commutation relations $[\varphi(x), \bar{\varphi}(y)] = 2\pi i$. In terms of the canonical Bose field $\Phi = \varphi + \bar{\varphi}$ and the dual field $\Theta = \varphi - \bar{\varphi}$ we find

$$\mathcal{H}' = \frac{\tilde{v}}{16\pi} \int dx [(\partial_x \Phi)^2 + (\partial_x \Theta)^2] . \quad (\text{E17})$$

The high-energy cutoff in this construction is given by the depth of the Fermi sea in the lower band of (E11), which is $H - m = H - H_c$. So far we have neglected the gap anisotropy, i.e. the term

$$\mathcal{H}_{\text{pair}} = i\Delta [\Psi_R^\dagger \Psi_L^\dagger - h.c.] \quad (\text{E18})$$

in the Hamiltonian (2.14). In the next step we take it into account under the assumption that Δ is small compared to the cutoff $H - H_c$. In this limit $\mathcal{H}_{\text{pair}}$ is expressed in terms of the modes as

$$\mathcal{H}_{\text{pair}} = i\Delta \int_{-\infty}^{\infty} \frac{dk}{2\pi} [c_R^\dagger(k) c_L^\dagger(-k) - c_L(-k) c_R(k)] . \quad (\text{E19})$$

After the Bogoliubov transformation this becomes

$$\begin{aligned} &-i\Delta \int_0^\infty \frac{dk}{2\pi} \cos(2\varphi_k) [d(k) d(-k) - c(k) c(-k) - h.c.] \\ &+ \text{mixed terms.} \end{aligned} \quad (\text{E20})$$

Dropping the ‘‘high-energy’’ filled band as well as the mixed terms (they contribute in higher orders of $\Delta/(H - H_c)$) we have

$$\mathcal{H}'_{\text{pair}} \simeq -i\Delta \int_0^\infty \frac{dk}{2\pi} \frac{vk}{\sqrt{m^2 + v^2 k^2}} [d(k) d(-k) - h.c.] . \quad (\text{E21})$$

Expanding around $\pm k_F$ this can be rewritten in terms of the left and right moving fermions as

$$\mathcal{H}'_{\text{pair}} \simeq i\Delta \sqrt{1 - \frac{m^2}{H^2}} \int dx [RL - L^\dagger R^\dagger]. \quad (\text{E22})$$

Finally, bosonization gives

$$\mathcal{H}'_{\text{pair}} \simeq -\frac{\Delta}{\pi} \sqrt{1 - \frac{m^2}{H^2}} \int dx \cos\left(\frac{\Theta}{\sqrt{2}}\right). \quad (\text{E23})$$

By combining Eqns (E17) and (E23) we see that in the absence of interactions the Majorana fermion model gives rise to a sine-Gordon effective theory at low energies in the parameter regime we have been discussing. The parameter β in (5.3) takes the special free-fermionic value $\beta = 1/\sqrt{2}$.

Interactions can be treated in a way analogous to the pairing term. If we drop the interaction terms involving the third Majorana (which we assume to have the largest gap) the interaction Hamiltonian reads

$$\mathcal{H}_{\text{int}} = 2g_3 \int dx L_1 L_2 R_1 R_2, \quad (\text{E24})$$

where $g_3 < 0$. Expressing this in terms of the complex fields $\Psi_{R,L}$, carrying out a mode expansion and subsequent Bogoliubov transformation and finally projecting to the low-energy band we obtain

$$\mathcal{H}'_{\text{int}} \simeq 2g_3 \frac{v^2 k_F^2}{m^2 + v^2 k_F^2} \int dx R^\dagger R L^\dagger L, \quad (\text{E25})$$

where R and L have been introduced in (E14). Bosonization then gives

$$\mathcal{H}'_{\text{int}} \simeq \frac{g'_3 \tilde{v}}{16\pi} \int dx [(\partial_x \Phi)^2 - (\partial_x \Theta)^2], \quad (\text{E26})$$

where $g'_3 = \frac{g_3 \tilde{v}}{\pi v^2}$. This term may be combined with (E17) by rescaling the scalar fields in the standard way

$$\Phi \longrightarrow \left[\frac{1 - g'_3}{1 + g'_3} \right]^{\frac{1}{4}} \Phi, \quad \Theta \longrightarrow \left[\frac{1 + g'_3}{1 - g'_3} \right]^{\frac{1}{4}} \Theta. \quad (\text{E27})$$

In terms of the rescaled fields the total Hamiltonian takes the form of a sine-Gordon model (5.3) (with a slightly changed velocity) where

$$\beta = \left[\frac{1 + g'_3}{1 - g'_3} \right]^{\frac{1}{4}} \frac{1}{\sqrt{2}} < \frac{1}{\sqrt{2}}. \quad (\text{E28})$$

Hence the sine-Gordon model is in the attractive regime.

APPENDIX F: CORRELATION AMPLITUDE IN THE COMMENSURATE-INCOMMENSURATE TRANSITION

Let us consider the LG model (3.1) in the U(1) symmetric case $\Delta_1 = \Delta_2 = \Delta_3 = m$. For $H > H_c = m$ the low-energy degrees of freedom are described by a Luttinger liquid, which can be derived by means of Haldane's harmonic fluid approach²⁵ as follows. Forming a complex Bose field out of the two components of the LG field that couple to the magnetic field

$$\Psi_B = \frac{\varphi_1 + i\varphi_2}{\sqrt{2}}, \quad (\text{F1})$$

and then bosonizing using²⁵

$$\Psi_B^\dagger \simeq \sqrt{\rho_0 + a_0 \Pi} \left[\sum_{m \text{ even}} e^{im\Theta} \right] e^{i\Phi}, \quad (\text{F2})$$

one obtains, after rescaling the fields Φ and Θ , a Lagrangian density of the form¹⁴

$$\mathcal{L} = \frac{1}{16\pi} \left[\frac{1}{\tilde{v}} \left(\frac{\partial\Theta}{\partial t} \right)^2 - \tilde{v} \left(\frac{\partial\Theta}{\partial x} \right)^2 \right]. \quad (\text{F3})$$

Here $\tilde{v} = 2v\sqrt{2\frac{H-m}{m}}$, ρ_0 is the (dimensionless) boson density, which corresponds to the magnetization per site and Π is the momentum conjugate to Φ . As the LG fields φ_a are the staggered components of the spin operators we conclude that

$$S_j^\pm \propto (-1)^j A \exp\left(\pm \frac{i\beta\Theta}{2}\right), \quad (\text{F4})$$

where β depends on the magnetization and is related to the parameter η of Ref. [14] by $\beta^2 = \eta$. By virtue of (F2) the amplitude A is proportional to

$$A \propto \sqrt{\rho_0} a^{\frac{\beta^2}{2}}, \quad (\text{F5})$$

where a is a short-distance cutoff and vertex operators are normalized according to (5.6). The short-distance cutoff is

$$a = \frac{a_0}{\rho_0}. \quad (\text{F6})$$

We note that the short-distance cutoff (F6) diverges as H approaches m as $\rho_0 \rightarrow 0$ and (F4) describes the asymptotic behaviour of spin correlation functions at distances much larger than a . Combining (F6) and (F5) we find that in general we have²⁵

$$A \propto \rho_0^{\frac{1-\beta^2}{2}} \quad (\text{F7})$$

Let us now specialize to magnetic fields very close to the critical field $H_c = m$

$$H - m \ll m. \quad (\text{F8})$$

As shown in Ref. [25], the parameter β tends to $\frac{1}{\sqrt{2}}$, so that

$$S_j^\pm \propto (-1)^j A \exp\left(\pm \frac{i\Theta}{2\sqrt{2}}\right), \quad (\text{F9})$$

where the density is given by¹⁴

$$\rho_0 = \frac{a_0}{\pi v} \sqrt{2m(H-m)}. \quad (\text{F10})$$

Combining (F10), (F6) and (F5) we obtain

$$A = A' a_0^{\frac{1}{4}} \left[\frac{H - H_c}{J} \right]^{\frac{1}{8}}, \quad (\text{F11})$$

where A' is a numerical, field independent constant and where we have used that $\frac{v^2}{ma_0^2} \propto J$. The field dependence of the correlation amplitude (F11) is a universal feature of the C-IC transition.

Let us apply these ideas to another example of the C-IC transition: the spin-1/2 Heisenberg XXZ chain in a longitudinal magnetic field

$$\begin{aligned} \mathcal{H}_{\text{XXZ}} = & J \sum_n S_n^x S_{n+1}^x + S_n^y S_{n+1}^y + \delta S_n^z S_{n+1}^z \\ & + H \sum_n S_n^z, \end{aligned} \quad (\text{F12})$$

where $-1 < \delta \leq 1$. The model (F12) has a phase transition from a gapless, incommensurate Luttinger liquid phase to a gapped, commensurate, spin-polarized phase at a critical value

$$H_c = J(1 + \delta). \quad (\text{F13})$$

Slightly below this transition, i.e.

$$0 < 1 - \frac{H}{H_c} \ll 1, \quad (\text{F14})$$

the transverse correlation functions exhibit the following large-distance asymptotics

$$\langle S_1^x(0) S_{R+1}^x(0) \rangle \sim (-1)^R \frac{e^{\frac{1}{2} 2^{\frac{11}{12}} ([H_c - H]/J)^{\frac{1}{4}}}}{4A^6 R^{\frac{1}{2}}}, \quad (\text{F15})$$

where A is Glaisher's constant (4.12). This result is obtained as follows: the dependence on the magnetic field is universal and given by (F11). The numerical coefficient is fixed by noting that the numerical results of Ref.[18] show that A' is independent of the value of the anisotropy δ . Finally, we use that the correlation amplitude has been calculated for the free fermion case in Ref.[47]. The result (F15) is in good agreement with the numerical results of Ref.[18] in the close proximity of the transition, as was already noted in¹⁸.

- ¹ F.D.M. Haldane, Phys. Rev. Lett. **50**, 1153 (1983).
- ² Y. Chen, Z. Honda, A. Zheludev, C. Broholm, K. Katsumata and S.M. Shapiro, Phys. Rev. Lett. **86**, 1618 (2001).
- ³ A. Zheludev, Z. Honda, Y. Chen, C. L. Broholm and K. Katsumata, Phys. Rev. Lett. **88**, 077206 (2002).
- ⁴ A. Zheludev, Z. Honda, C.L. Broholm, K. Katsumata, S.M. Shapiro, A. Kolezhuk, S. Park and Y. Qiu, Phys. Rev. **B68**, 134438 (2003).
- ⁵ A. Zheludev, S. M. Shapiro, Z. Honda, K. Katsumata, B. Grenier, E. Ressouche, L.-P. Regnault, Y. Chen, P. Vorderwisch, H.-J. Mikeska and A. K. Kolezhuk, Phys. Rev. **B69**, 054414 (2004).
- ⁶ H. Tsujii, Z. Honda, B. Andraka, K. Katsumata and Y. Takano, preprint cond-mat/0409190.
- ⁷ M. Hagiwara, Z. Honda, K. Katsumata, A. K. Kolezhuk and H.-J. Mikeska, Phys. Rev. Lett. **91**, 177601 (2003).
- ⁸ A. Zheludev, Z. Honda, K. Katsumata, R. Feyerherm and K. Prokes, Europhys. Lett. **55**, 868 (2001).
- ⁹ H.J. Schulz, Phys. Rev. **B34**, 6372 (1986).
- ¹⁰ I. Affleck, Phys. Rev. **41**, 6697 (1990).
- ¹¹ G. I. Dzhaparidze and A. A. Nersisyan, JETP Lett. **27**, 224 (1978), V. L. Pokrovsky and A. L. Talapov, Phys. Rev. Lett. **42**, 65 (1979), H.J. Schulz, Phys. Rev. **B22**, 5274 (1980).
- ¹² A. Furusaki and S.C. Zhang, Phys. Rev. **B60**, 1175-1187 (1999).
- ¹³ R. Konik and P. Fendley, Phys. Rev. **B66**, 144416 (2002).
- ¹⁴ I. Affleck, Phys. Rev. **B43**, 3215 (1991).
- ¹⁵ A.M. Tselik, Phys. Rev. **B42**, 10499 (1990).
- ¹⁶ J. Lou, S. Qin, T.-K. Ng, Z. Su, and I. Affleck, Phys. Rev. **B** 62, 3786 (2000).
- ¹⁷ L. Campos Venuti, E. Ercolessi, G. Morandi, P. Pieri, M. Roncaglia, Int. Jour. Mod. Phys. **B16**, 1363 (2002).
- ¹⁸ A. Furusaki and T. Hikihara, Phys. Rev. **B69**, 064429 (2004).
- ¹⁹ E.H. Lieb and W. Liniger, Phys. Rev. **130**, 1605 (1963).
- ²⁰ T.T. Wu, B.M. McCoy, C.A. Tracy and E. Barouch, Phys. Rev. **B13**, 316 (1976).
- ²¹ V.P. Yurov and A.I.B. Zamolodchikov, Int. Jour. Mod. Phys. **A6**, 3419 (1991).
- ²² J.L. Cardy and G. Mussardo, Nucl. Phys. **B340**, 387 (1990).
- ²³ F.H.L. Essler, Phys. Rev. **B62**, 3264 (2000).
- ²⁴ S. Sachdev, "Quantum Phase Transitions", Cambridge University Press, Cambridge (1999).
- ²⁵ F.D.M. Haldane, Phys. Rev. Lett. **47**, 1840 (1981).
- ²⁶ Y.J. Wang, preprint cond-mat/0306365.
- ²⁷ A.B. Zamolodchikov, JETP Lett. **25**, 468 (1977); H.-J. Thun, T.T. Truong, P.H. Weisz, Phys. Lett. **B67**, 321 (1977).
- ²⁸ F.A. Smirnov, *Form Factors in Completely Integrable Models of Quantum Field Theory* (World Scientific, Singapore, 1992).
- ²⁹ S. Lukyanov, Mod. Phys. Lett. **A12**, 2911 (1997).
- ³⁰ D.J. Scalapino, Y. Imry and P. Pincus, Phys. Rev. **B11**, 2042 (1975).
- ³¹ T. Sakai and M. Takahashi, Phys. Rev. **B42**, 4537 (1990).
- ³² B.M. McCoy and T.T. Wu, Phys. Rev. **D18**, 1259 (1978).
- ³³ B.M. McCoy and T.T. Wu, Phys. Rev. **B18**, 4886 (1978).
- ³⁴ G. Delfino, G. Mussardo and P. Simonetti, Nucl. Phys. **B473**, 469 (1996).
- ³⁵ T. Sakai and M. Takahashi, Phys. Rev. **B43**, 13383 (1991).
- ³⁶ S.T. Carr and A.M. Tselik, Phys. Rev. Lett. **90**, 177206 (2003).
- ³⁷ A.B. Zamolodchikov, Int. Jour. Mod. Phys. **A4**, 4235 (1989).
- ³⁸ G. Delfino and G. Mussardo, Nucl. Phys. **B455**, 724 (1995).
- ³⁹ D.J. Scalapino, Y. Imry and P. Pincus, Phys. Rev. **B11**, 2042 (1975).
- ⁴⁰ S. Allen and D. Loss, Physica **A239**, 47 (1997), B. Normand, J. Kyriakidis and D. Loss, Ann. Phys. **9**, 133 (2000).
- ⁴¹ M.D.P. Horton and I. Affleck, Phys. Rev. **B60**, 9864 (1999).

- ⁴² A.B. Zamolodchikov and Al.B. Zamolodchikov, *Annals of Physics* **120**,253 (1979).
- ⁴³ V.A. Fateev, *Phys. Lett.* **B324**, 45 (1994).
- ⁴⁴ H. Bergknoff and H. Thacker, *Phys. Rev.* **D19**, 3666 (1979), V.E. Korepin, *Theor. Math. Phys.* **41**, 169 (1979).
- ⁴⁵ D.J. Gross and A. Neveu, *Phys. Rev.* **D10**, 3235 (1974).
- ⁴⁶ P. Fonseca and A.B. Zamolodchikov, preprint hep-th / 0309228.
- ⁴⁷ H.G. Vaidya and C.A. Tracy, *Physica* **92A**, 1 (1978).